DOE/ER/60674--3

DE91 004591

DOE/ER/60674-3

BASE SEQUENCE EFFECTS ON INTERACTIONS OF AROMATIC MUTAGENS WITH DNA

Comprehensive Progress Report

for the period March 1, 1988 - August 31, 1990

N.E. Geacintov

New York University
New York, New York 10003

August 31, 1990

Prepared for

THE U.S. DEPARTMENT OF ENERGY
AGREEMENT NO. DE-FG02-88ER60674

SUMMARY

The characteristics and base sequence-dependence of the binding of the tumorigenic (+)-anti-benzo[a]pyrene-7,8-diol-9,10-oxide (BPDE) and the non-tumorigenic (-)-isomer to nucleic acids have been determined. The sequence- and isomer-dependent covalent binding by *cis* and *trans* addition to the exocyclic amino-group of guanine has been established in synthetic polynucleotides and oligonucleotides of defined base composition and sequence. The *cis* and *trans* addition products give rise to DNA adducts of different conformations, which appear to be important determinants of the biological activities of this class of energy-related chemicals.

TABLE OF CONTENTS

INTRODUCTION AND OVERVIEW

This report is a summary of research performed during the period March 1, 1988 to August 31, 1990 and supported by DOE Grant No. DE-FG02-88ER60674. This three-year project period expires on February 28, 1991.

Significance. This work is concerned with a class of energy-related chemicals, the polycyclic aromatic hydrocarbons (PAH), which are known to be carcinogenic in mammals and are mutagenic in prokaryotic test systems. The PAH compounds are by-products of combustion of fossil fuels and are emitted into the environment, thus constituting an important potential health hazard. *In vivo*, they are activated metabolically to reactive epoxide intermediates which bind noncovalently and covalently to DNA, the genetic material of the cell. The formation of DNA adducts gives rise to mutations, and is believed to be the key initial event in the complex, multi-stage tumorigenesis process.

General Objectives. The development of techniques for a thorough understanding, on a molecular level, of the mechanisms of action of mutagenic and tumorigenic PAH epoxide metabolites. Differentiate the mechanisms by which these biologically active compounds and their inactive isomers damage DNA, and the differences in the biological end-points produced. Develop new and sensitive techniques for monitoring the presence of biologically deleterious and benign PAH-DNA lesions in cellular DNA.

Specific Objectives for this Project Period. Determine the physico-chemical aspects of non-covalent complex formation, chemical reactivity, and covalent adduct formation of selected PAH model metabolite model compounds with polynucleotides and oligonucleotides of defined base composition and sequence. In this project period, special emphasis is placed on the development of methods for recognizing specific base-sequence effects which might be important in distinguishing active and inactive isomers of PAH epoxide derivatives.

Summary of Major Accomplishments. The highlights of the results of this most recent project period point to several promising future directions of research. The major results can be summarized as follows:

(1) The PAH metabolites (derived from benzo[a]pyrene) bind noncovalently to DNA. Base-sequence effects are of minor importance to the biologically critical reaction with guanine, since these metabolites hop from site to site on the DNA molecule on millisecond time scales before binding chemically to one of the guanines.

(2) Fluorescence methods can distinguish between intercalative, base-stacking, and exterior type carcinogen-DNA adduct conformations in the single- and double-stranded forms.

(3) The covalent binding of benzo[a]pyrene-7,8-diol-9,10-epoxides (BPDE) to runs of guanines gives rise to well-oriented and physically well-defined adducts. The presence of the more flexible dA-dT base pairs near the BPDE-guanine lesions substantially lowers the degree of orientation, an effect attributed to the lower stabilities, higher flexibilities, and breathing rates of dA-dT base pairs. The higher rigidities and defined orientations of the carcinogens in runs of dG-dC base pairs may give rise to the observed preference of mutations in runs of G's in cellular DNA.

(4) The most important achievement from the point of view of future advances, is our success in synthesizing site-specific BPDE-oligonucleotide adducts with any desired base surrounding a BPDE-guanine (or adenine) lesion. Initial spectroscopic and thermodynamic studies have already yielded fascinating new data.

(5) Stereochemically different *cis* and *trans* addition products are related to the different site I and site II adducts, observed by us previously in heterogeneous adducts obtained with high molecular DNA. Since Site II adducts are associated with the most tumorigenic PAH diol epoxide derivatives, while site I adducts are associated with the least active metabolites, we tentatively associate high biological activity with the formation of site II, *trans* adducts.

(6) The above hypothesis, in part, accounts for the differences in tumorigenic activities of the stereoisomers of *anti*-BPDE. The (+)-enantiomer forms predominantly *trans* (site II) adducts, while the (-)-isomer forms predominantly *cis* (site I) adducts.

(7) Thermodynamic studies show that the non-tumorigenic (-)-BPDE isomer upon covalent binding, strongly destabilizes DNA duplexes, while the effect of the tumorigenic (+)-enantiomer is small. These differences may result in differential response of repair and replication enzymes, thus accounting for the differences in the biological activities of these two isomers, which are merely mirror images of one another.

(8) Electrophoretic Maxam-Gilbert gel mobility studies suggest that covalent (+)-*trans*-BPDE-dG lesions give rise to a bend or flexible hinge joint at the site of binding. The other stereochemically different BPDE adducts do not.

Organization of this Progress Report. This report stresses only those results which have not yet been published. Part I describes thermodynamic and kinetic studies of the binding of PAH metabolites to DNA. Part II describes the characteristics of covalent BPDE-dG adducts as a function of base-sequence. Each subsection is accompanied by a detailed list of conclusions which serve to amplify the summary provided above.

A list of personnel associated with this grant is given at the end of this report. A list of publications and manuscripts in preparation is also included.

PART I: MECHANISMS OF INTERACTION AND BINDING OF POLYCYCLIC AROMATIC HYDROCARBON METABOLITES WITH NUCLEIC ACIDS.

A. Thermodynamics of physical complex formation as a function of size and structure of PAH metabolites.

It is interesting to note that the dimensions of the most tumorigenic PAH compounds are limited to molecules with 4-6 condensed aromatic rings [1]. One might speculate that larger PAH molecules are either insoluble in the aqueous cellular environment, or are too large to fit into DNA binding sites. Smaller molecules on the other hand, are probably characterized by higher affinities for the aqueous environments than the larger PAH derivatives, and their affinities for DNA binding sites should therefore be correspondingly lower. Molecular size may also play a role during DNA synthesis at replication forks; the $\pi - \pi^*$ stacking interactions between PAH residues bound covalently to a particular base with neighboring purine and pyrimidine moieties, may provide an additional impediment to the normal functioning of the polymerases [2,3]. Furthermore, it has been shown experimentally that BPDE binds noncovalently and intercalatively to native double-stranded DNA before undergoing the covalent binding reaction [4-6]. In order to investigate the thermodynamic factors which govern the physical association of PAH derivatives of different structures with DNA bases, we studied the equilibrium association constants **K** as a function of temperature. The reversible equilibrium between free (PAH) and DNA-bound (complex) molecules is:

$$\text{PAH} + \text{DNA} \underset{k_2}{\overset{k_1}{\rightleftharpoons}} [\text{complex}] \qquad [1]$$

where k_1 and k_2 are the bimolecular association and unimolecular dissociation rate constants, respectively. The association constant is defined as:

$$K = \frac{k_1}{k_2} \qquad [2]$$

We have previously investigated the variations of **K** of the diol epoxide BPDE (Fig. 1) as a function of base composition and sequence utilizing synthetic polynucleotides [7].

The temperature dependence of the equilibrium constant **K** is, as usual, described by the van't Hoff relationship:

$$\ln K = \frac{\Delta H^o}{R}\frac{1}{T} - \frac{\Delta S^o}{R} \qquad [3]$$

Which thermodynamic factors constitute the driving force for the noncovalent complexation between mutagenic PAH molecules and nucleic acids? This question can be answered by studying the temperature dependence of PAH diol epoxides to nucleic acids as a function of temperature, and determining the enthalpy and entropy changes from van't Hoff plots. However, because diol epoxide derivatives are unstable in aqueous solutions, it is easier (and more accurate results are obtained) to work

with the diol or tetraol hydrolysis products of PAH epoxide or PAH diol epoxide derivatives [8-11].

Our original plan was to study the temperature dependence and ionic strength dependence of K for a representative tetraol (BPT) in polynucleotides of different base composition and sequence. However, during the course of this work, an excellent study by Shimer et al. [10] was published. We therefore proceeded to the second phase of our project to study the thermodynamics of binding of phenolic PAH metabolites of different structures to DNA. Native DNA was selected because of cost, and because the binding of the diol epoxide BPDE to polymers of different base sequences and to random sequence DNA appears to be qualitatively similar, although the values of K are quite different in different base sequences [7].

In studying the temperature dependence of K, we utilized the fluorescence quenching method of LeBreton [8], which provides correct values of K under certain experimental conditions [9-11]. All diols and tetraols studied were obtained by hydrolyzing the racemic epoxides in aqueous solutions, and subsequently purifying the *cis* and *trans* hydrolysis products by reverse phase HPLC (C_{18} column), utilizing a 60-100% methanol/water gradient. In some cases, we have not yet had the opportunity to definitively identify the earlier (#1) or later-eluting (#2) HPLC peaks as either *cis* or *trans*. Typical van't Hoff plots for the series of molecules depicted in Fig. 1, are shown in Fig. 2. The enthalpy and entropy parameters are summarized in Table 1. The association constant K in the case of the 1,2,3,4-tetrahydroxytetrahydro-benz[a]anthracene (BAT) was too small for accurate temperature-dependent measurements.

TABLE 1. *Thermodynamic parameters of physical binding to native, double-stranded DNA in 5 mM Tris buffer, pH 7.9.*

Compound	K (25°C)	ΔH°	ΔS°	$(\Delta H^\circ/T\Delta S^\circ)^*$
1-OP (diol)	2800	-8.4	-6.1	4.6
9,10-BPH_4D (diol) (*cis*)	3400	-9.0	-7.0	4.3
9,10-BPH_4D (diol) (*trans*)	1700	-8.0	-6.0	4.5
BPT (tetraol) (*trans*)	1500	-7.4	-5.2	4.8
3-MCT (tetraol) (HPLC peak #1)	660	-4.8	-1.5	11.0
7-MeBA (tetraol) (HPLC peak #1)	400	-7.0	-5.7	4.1
7-MeBA (tetraol) (HPLC peak #2)	130	-11.0	-14.0	2.6
BAT (tetraol) (*trans*)	55	---	---	

K is in units of M^{-1}, ΔH^{o} in units of kcal/mol, and ΔS^{o} in units of cal deg^{-1} mol^{-1}. All thermodynamic values within ± 5%.
*Evaluated at 298 K.

The following conclusions can be reached from the data in Table 1:

1. The association constants K are generally larger for systems containing four aromatic rings than for those containing three aromatic rings. These results suggest that the noncovalent association constants depend, at least in part, on the size of the aromatic ring system. The magnitudes of K are strongly dependent on the experimental conditions, especially ionic strength, and thus comparisons between values reported from different laboratories are difficult. Nevertheless, the values of K shown in Table 1 are similar to those reported elsewhere for BPT and 7-MeBA tetraol derivatives [7-12].

2. Alkyl substitution, especially at the 7-position of BA, enhances the magnitude of K, an effect which is attributed to an enhancement of the polarizability of the aromatic molecules induced by the presence of the methyl group [12].

3. The data in Table 1 clearly shows that the magnitude of K depends on the stereochemical characteristics of the diols and tetraols. These findings are similar to those we reported previously for stereoisomeric BPDE diol epoxides, which showed that K is smaller for *syn* than for *anti* diastereomers [13]. After identification of the appropriate HPLC elution peaks (Table 1), and completing our studies with *cis*-BPT, and in conjunction with computer modeling docking studies, we hope to obtain a deeper understanding of this dependence of K on steric factors.

4. The ΔH^{o} values, except for one of the 7-MeBA isomers (HPLC peak #2) tend to be smaller for molecules with anthracenyl chromophores than for those with pyrenyl chromophores. This difference may be due to increased base-stacking interactions in the latter cases, although steric considerations can modify such interactions. The ΔH^{o} values are, overall, in the same range as those reported for *trans*-9,10-BPH_2-diol and (±)-*anti*-BPDE [9] in calf thymus DNA, and *trans*-BPT in some synthetic polynucleotides [10]. These ΔH^{o} and ΔS^{o} values are typical of polycyclic aromatic intercalators [9,10]. Recent evidence suggests that BPT [5,6] and BA derivatives 14] do bind noncovalently to native DNA by an intercalation mechanism, while 3-MC derivatives [14] do not.

5. With the exception of the 3-MCT and 7-MeBA (peak #2) tetraols, the ratio of $\Delta H^{o}/T\Delta S^{o}$ ratio is fairly constant and lies in the range of 4.1 - 4.8, indicating that enthalpic factors are more important than entropic factors in determining the magnitude of the physical association constant K at 25° C.

6. The changes in entropy upon physical complex formation are negative in sign, in agreement with other studies [9,10]. Thus, entropy factors do not favor the formation of noncovalent PAH metabolite-DNA complexes. The lowering in entropy is believed to be associated with the release of counter ions from DNA binding sites: intercalative complex formation leads to a further separation between neighboring negatively charged phosphate groups, which allows for a

partial release of Na^+ counter ions. Hydration of these counter ions is accompanied by large negative entropy changes. Counteracting this negative contribution to the entropy change, the release of presumably structured water molecules surrounding the PAH molecules in solution, should give rise to a positive entropy contribution upon intercalation (classical hydrophobic effect).

7. The 3-MCT tetraol is characterized by unusually low values of ΔH^o and ΔS^o. We have provided evidence that 3-MCDE molecules bind to the surface of native DNA and do not form intercalation complexes [14]. In an external binding geometry, both the enthalpic and entropic changes should be smaller than in the case of intercalation. The unusually high values of the enthalpy and entropy changes in the case of the 7-MeBA tetraol (HPLC peak 2) cannot be accounted for at this time.

In summary, our thermodynamic binding studies with PAH metabolite model compounds of different structures have shown, for the first time, that these parameters are strongly influenced by the stereochemistry of these molecules, and that intercalative and external DNA binding modes are characterized by very different values of ΔH^o and ΔS^o.

B. MECHANISMS AND BASE SEQUENCE DEPENDENCE OF NONCOVALENT AND COVALENT BINDING.

It is by now well established that the biologically important covalent binding reaction with DNA is preceded by the formation of noncovalent PAH diol epoxide DNA complexes [4-8]. In the case of BPDE, the ultimate mutagenic and carcinogenic form of the environmental pollutant benzo[a]pyrene, there is a definite preference for forming *physical* or *noncovalent* intercalative complexes at alternating (dA-dT)•(dA-dT) sites [7]. On the other hand, the dominant and biologically critical chemical binding reaction of BPDE, occurs preferentially at dG in native DNA [1]. The magnitudes of the physical association constants K and f_{cov}, the relative efficiencies of forming covalent adducts (fraction of BPDE molecules which react covalently with the nucleic acid molecules), are summarized in Fig. 3 for polynucleotides of different base composition and sequence. It is remarkable that poly(dA-dT)•(dA-dT) exhibits a large K value, and also a low value of f_{cov}. There seems to be no direct relationship between noncovalent binding and covalent adduct formation, as is often assumed [8]. In order to account for this apparent paradox, we have postulated that free BPDE is in equilibrium with noncovalently complexed BPDE, and that the BPDE-DNA complexes are formed and dissociate on millisecond, or submillisecond time scales. Since, typically, the covalent binding reaction takes place on time scales of minutes, this model suggests that a BPDE molecule can sample many different noncovalent binding sites during its lifetime of several minutes [7].

In order to demonstrate this point experimentally, we studied the kinetics of binding and dissociation of BPT, the chemically stable hydrolysis product of BPDE, using native DNA and various synthetic polynucleotides. The tetraol BPT was employed in these studies, rather than the diol epoxide BPDE, because it is difficult to perform repetitive kinetic experiments with the unstable diol epoxide molecules. We utilized the triplet excited state techniques developed in our laboratory earlier [15,16], in order to study the equilibrium:

$$
\begin{array}{ccc}
{}^3\mathrm{BPT}^* + \mathrm{DNA} & \underset{k_2}{\overset{k_1}{\rightleftharpoons}} & [{}^3\mathrm{BPT}^*\text{-DNA}]_{\mathrm{complex}} \\
\Big\downarrow k_f & & \Big\downarrow k_c \\
\mathrm{BPT} & & [\mathrm{BPT} - \mathrm{DNA}]_{\mathrm{complex}}
\end{array}
\qquad [4]
$$

where k_1 and k_2 are the rate constants of formation and dissociation of the complexes, k_f and k_c are the rate constants of decay of the free and complexed photoexcited triplet states ${}^3\mathrm{BPT}^*$, respectively. The point of these experiments is that the lifetimes of the complexes, k_2^{-1}, denote the average time that a given BPT molecule spends at a particular DNA intercalation site. This approach involves the use of a flash photolysis apparatus to measure the kinetics of the ${}^3\mathrm{BPT}^*$ triplet decay. Following excitation with a strong xenon flash, the triplet excited molecules display a transient absorption spectrum with a maximum at 420 nm which decays in the μs - ms time range. Based on the above reaction scheme, a set of coupled differential equations can be written to describe the time dependence of the concentration of bound and free BPT molecules. The solutions of these equations indicate that ${}^3\mathrm{BPT}^*$ should decay according to bi-exponential kinetics [15]:

$$[{}^3\mathrm{BPT}^*(t)]_{(\mathrm{free\ +\ complexed})} = A_1\exp[-\Gamma_1 t] + A_2\exp[-\Gamma_2 t] \qquad [5]$$

where Γ_1 and Γ_2 are decay constants which depend on the DNA concentration, and on the rate constants k_1, k_2, k_A, and k_c [15]. The amplitudes A_1 and A_2 depend on the relative fractions of bound and free BPT molecules at time t=0, and other factors. Several different experimental cases can be distinguished from the decay kinetics of triplet excited states:

(1) Only one decay component is observed, rather than two. This means that the lifetime k_2^{-1} of complexed BPT molecules at a given DNA binding site is much shorter than the intrinsic lifetime k_c^{-1} of triplet molecules at these sites ($k_2 >> k_c$. This is the situation observed in the case of the cationic dyes acridine orange an proflavine [15]. Physically, this means that the molecules exchange DNA binding sites many times before they decay.

(2) Two decays are observed with lifetimes characteristic of free and bound molecules, which are equal to $\Gamma_1^{-1} = k_A^{-1}$ and $\Gamma_2^{-1} = k_C^{-1}$, respectively. There is no exchange at all between free and bound molecules during the lifetimes of the excited triplets.

(3) The decay constants Γ_1 and Γ_2 are different from one another and vary with the DNA concentration. In this case the magnitude of k_2 is comparable to that of k_C. Exchange is occurring during the lifetimes of the triplets.

Our experimental data show that case (3) appropriately describes the binding equilibrium of ${}^3\mathrm{BPT}^*$ to different polynucleotides in aqueous solutions (to be published). Thus, BPT molecules exchange binding sites during their lifetimes of 3 - 20 ms in DNA solution. A detailed analysis of the decay curves and other parameters indicate that the rate constants shown in scheme [4] above, are different for polynucleotides of different base composition and sequence. The results of these curve-fitting methods are summarized in Table 3.

The monomeric nucleosides deoxyadenosine (dA), deoxyguanosine (dG), deoxycytidine (dC), and thymidine (dT), also quench $^3BPT^*$, though with different efficiencies (different values of the bimolecular quenching constant k_1).

TABLE 3. Base-sequence dependence of BPT-DNA complex dissociation constant k_2, quenching constant k_1, and triplet ($^3BPT^*$) lifetimes $\tau = k_C^{-1}$ (or k_A^{-1}) from analysis of triplet decay kinetics (All values ± 10%).

Polymer	k_1, $M^{-1}s^{-1}$	k_2^{-1}, ms	τ, ms
None	--	--	3.0
Group I			
Calf thymus DNA	5.9×10^6	3.6	16
poly(dG-dC)•(dG-dC)	1.8×10^6	3.1	18
poly(dG)•(dC)	1.8×10^6	3.8	16
Group II			
poly(dA)(dT)	7.8×10^5	10	4.8
poly(dA-dT)•(dA-dT)	1.0×10^6	14	4.3
poly(dA-dG)•(dT-dC)	1.5×10^6	25	3.9
poly(dA-dC)•(dT-dG)	3.4×10^6	9.0	5.6
Monomers			
dA	5.0×10^5	--	
dC	1.3×10^5	--	
dG	1.0×10^5	--	
dT	5.7×10^4	--	

The following conclusions are reached:

(1) The results can be grouped into two different categories; Group I includes DNA and both dG-dC polymers, while Group II contains all of the synthetic polynucleotides with dA-dT base pairs.

(2) In group I the residence time of BPT molecules at a particular binding site is less than 4 ms.

(3) In group II, the residence time is longer (> 9 ms).

(4) Adenosine quenches the triplet excited states of BPT more than either dG or dC. This may account for the shorter lifetimes ($\tau = k_C^{-1}$) of triplets bound to the polymers which contain dA-dT base pairs (Group II), rather than dG-dC base pairs only (DNA is an exception).

(5) Complexes are not formed with the individual nucleoside monomers, i.e. are not detectable by the triplet kinetic method. Thus, complex formation requires an intact secondary polymer structure.

(6) Base-sequence effects on k_2 are small, although distinctly different for group I and group II polymers. It is reasonable to assume that the behavior of BPDE molecules is similar to that of the tetraol hydrolysis products. An upper limit of the residence time of a molecule at a particular physical binding site is $\approx$ 25 ms.

(7) These findings provide a rationale for the difference between the physical binding constants K and the covalent binding parameter f_{cov}. There need not be a correlation between these two quantities since the polycyclic molecules hop from binding site to binding site many times before undergoing a chemical binding reaction with the exocyclic amino group guanosine.

CONCLUSIONS

The formation of noncovalent intercalation complexes prior to covalent binding is not a critical requirement for the biological action of this class of PAH diol epoxide molecules. In our subsequent studies, we have therefore focused our efforts on the nature of the covalent addition products.

PART II

A. DNA BASE SEQUENCE DEPENDENCE OF CONFORMATIONS OF COVALENT DEOXYGUANOSINE ADDUCTS DERIVED FROM STEREOISOMERIC BENZO[a]PYRENE DIOL EPOXIDES OF DIFFERENT TUMORIGENICITIES.

Biological Activity and Adduct Conformation.

The differences in the tumorigenicities and mutagenicities of the two enantiomers of trans-7,8-dihydroxy-anti-9,10-epoxy-7,8,9,10-tetrahydrobenzo[a]pyrene (BPDE) have been well documented [17]. Both enantiomers are known to bind predominantly to the exocyclic amino group of deoxyguanosine in DNA, although the (-)-enantiomer binds significantly to deoxyadenosine residues as well [18, and references therein]. Brookes and Osborne [19] concluded that the differences in biological activities are related to spatial differences in adduct conformations, and therefore differences in the processing of these lesions in a cellular environment.

DNA adduct conformations derived from BPDE and similar molecules can be classified according to the site I - site II hypothesis [20-22]. Site II adducts are characterized by an external, solvent-exposed conformation [23], while site I complexes involve considerable carcinogen-base stacking interactions. Physicochemical experiments with the (+)- and (-)-*anti*-BPDE enantiomers bound covalently to DNA have shown that the more tumorigenic (+)-enantiomer prefers a site II conformation, while the (-)-enantiomer exhibits predominantly site I-type conformations [22,24]. Several studies of BPDE adduct spectra (location of adducts as a function of base sequence) and mutation spectra (position within the DNA sequence where mutations occur) suggest that the binding of the tumorigenic (+)-*anti*-BPDE isomer to sequences rich in dG-dC base pairs, particularly those containing runs of dG's, may be of particular significance [25-28]. Using the synthetic polynucleotides poly(dG).(dC), poly(dG-dC).(dG-dC), poly(dA-dC).(dT-dG), and poly(dT-dC).(dA-dG), we have studied the base-sequence dependence of (1) the relative abundance of *cis* and *trans* addition products resulting from the binding of (+)-*anti*-BPDE and (-)-*anti*-BPDE to N(2) of dG, and (2) the relative abundance of site I/site II adduct conformations Absorbance and flow linear dichroism techniques were employed to distinguish between site I and site II adduct conformations. The principles of these techniques for distinguishing between these different types of adducts have been described [21,24]. The linear dichroism (LD) is defined as:

$$LD = A_{\parallel} - A_{\perp} \qquad [6]$$

where $A_{\parallel} - A_{\perp}$ are the absorbances measured with the electric vector of the polarizer oriented parallel and perpendicular, respectively, with respect to the preferred orientation of the DNA helical axis in the flow gradient in a Couette cell [21].

The *cis* and *trans* nature of the covalent BPDE-dG adducts was examined by the usual methods of enzyme digestion of the polynucleotides to the nucleoside level as previously described [18]. In this work we have, for the first time, correlated the stereochemically different *cis* and *trans* adducts (defined in Fig. 13) with site I and site II adduct conformations. This was first achieved qualitatively by a comparison of physical conformations and chemical adduct structures in

polynucleotides of different base composition using (+)-*anti*-BPDE and (-)-*anti*-BPDE, and finally from detailed studies of BPDE-oligonucleotide adducts.

Site I and Site II Absorption Spectra and Linear Dichroism Spectra.

Typical site I and site II absorption spectra derived from model systems are depicted in Fig. 4 (Site I spectrum: noncovalent (+)-BPDE-DNA complex; Site II: (+)-BPDE-poly(dG-dC).(dG-dC) adduct (solid line), and (+)-BPDE-dG monomer adduct (dotted line)). Site I spectra are characterized by red-shifted absorption maxima at 337 and 354 nm (significant carcinogen-base stacking interactions), while the maxima for the solvent-exposed site II adducts are located at 330 and 346 nm. The corresponding LD spectra are similar in shape to the absorption spectra (Fig. 1); for site I spectra the LD signal is negative, because the BPDE pyrenyl residues tend to be oriented perpendicular to the DNA axis, while for site II adducts the LD spectrum is positive in sign.

Characteristics of BPDE-poly(dG)•(dC) and BPDE-poly(dG-dC).(dG-dC) Adducts.

The absorption and linear dichroism spectra of covalent adducts derived from the binding of (+)-*anti*-BPDE and (-)-*anti*-BPDE to the poly(dG).(dC) homopolymer are clearly of the site II- and site I-type, respectively (Fig. 5). The LD spectrum of the (+)-adducts, while predominantly positive, exhibits a small minimum at about 360 nm. We conclude that the (+)-adducts are predominantly of the site II-type, but with a small contribution from site I adducts.

The characteristics of the (-)-*anti*-BPDE- and (+)-*anti*-BPDE-poly(dG-dC).(dC-dG) adducts are similar to those obtained with the homopolymer poly(dG).(dC). However, in the (-)-adduct, there is a sharp valley between the negative LD minima at 338 and 353 nm (Fig. 6); this suggests a contribution of a positive site II LD signal to the overall LD spectrum.

Characteristics of BPDE-poly(dA-dC).(dT-dG) and BPDE-poly(dT-dC).(dA-dG) Adducts.

In the case of the non-alternating pyrimidine-purine co-polymer poly(dT-dC).(dA-dG), the (-)-enantiomer seems to predominantly give rise to site I adducts, while the (+)-enantiomer gives rise to a mixture of site I and site II conformations as is evident from the LD spectra (Fig. 7).

In the case of the alternating pyrimidine-purine copolymer (-)-*anti*-BPDE-poly(dT-dG).(dA-dC) adduct, the absorption spectrum suggests a site I-type conformation since the broad absorption maxima are located at 337 and 352 nm (Fig. 8A). However, there is no detectable LD signal (Fig. 8C). The (+)-*anti*-BPDE-poly(dT-dG).(dA-dC) adducts are clearly heterogeneous in nature and the broad and weakly discernable maxima appear near 335 and 352 nm (Fig. 8B), while the LD minima are located at 338 and 358 nm (Fig. 8D). The (+)-*anti*-BPDE enantiomer appears to predominantly give rise to site II rather than to site I adducts ***only in this particular base sequence.***

HPLC Analysis of Covalent Adducts.

The higher incidence of site I conformations in the (+)-anti-BPDE-poly(dT-dG).(dA-dC) adducts might, in principle, be due to differences in the chemical nature of the adducts. We have therefore compared the adduct distributions in the (+) and (-)-adducts of poly(dG-dC)•(dG-dC) and poly(dG)•(dC), as well as (+)-anti-BPDE-poly(dT-dG).(dA-dC) and (+)-anti-BPDE-poly(dT-dC).(dA-dG) adducts. Some representative HPLC profiles are shown in Fig. 9; sensitive fluorescence detection (excitation at 345 nm, viewing at 380 nm) methods were employed in order to utilize smaller amounts of materials (the BPDE enantiomers are very expensive, and so are the polynucleotides). This fluorescence method was carefully calibrated by comparing the absorbance and fluorescence signals of standard [18] *trans* and *cis* (+)-BPDE-N(2)-dG, and (-)-BPDE-N(2)-dG adducts as they were eluted in the water/methanol gradients (reverse phase C_{18} columns). The *trans*/*cis* adduct ratios in the different polymers are summarized in Table 3. *Trans* adducts dominate in the case of the (+)-enantiomer in all cases, whereas in the case of (-)-BPDE, the abundance of *cis*-adducts is ≈ 1.5 - 2.5 times higher than that of *trans*-N(2)dG-adducts.

TABLE 3. *Trans/cis* BPDE-N(2)-dG adduct ratios

Polynucleotide	*(+)-BPDE*	*(-)-BPDE*
(dG)•(dC)	4.0	0.7
(dG-dC)•(dG-dC)	4.0	0.4
(dT-dC)•(dA-dG)	> 10	n.m.
(dA-dC)•(dT-dG)	> 10	n.m.

---

n.m..: not measured due to low reaction yields.
Reproducibility: ± 20%.

Average Orientation Angles of Pyrenyl Residues in Different Base Sequences.

The angle of orientation θ between a given transition moment and the reference axis in the LD experiment (in this case the flow direction within the Couette cell) is given by:

$$LD = (3/2)\, A\langle 3\cos^2\theta - 1\rangle F(G) \qquad [7]$$

where LD and A are the magnitudes of the linear dichroism and absorbances at one and the same wavelength, and $0 \le F(G) \le 1.0$ is a factor which expresses the degree of alignment of the polynucleotide. The average orientation of the long axes of the pyrenyl residues relative to the average orientations of the DNA bases can be estimated by comparing the reduced dichroism LD/A measured within the DNA absorption band and within the BPDE absorption band according to the equation [22]:

$$A' = \frac{(LD/A)_{BPDE}}{(LD/A)DNA} = \frac{\langle 3\cos^2\theta_{BPDE} - 1\rangle}{\langle 3\cos^2\theta_{DNA} - 1\rangle} = \langle 1 - 3\cos^2\theta_{BPDE}\rangle \qquad [8]$$

where the angle $\theta_{DNA} = 90^{\circ}$. Experimental values of A' and the apparent orientation angles θ_{BPDE} deduced therefrom are summarized in Table 4.

where the angle $\theta_{DNA} = 90^{o}$. Experimental values of A' and the apparent orientation angles θ_{BPDE} deduced therefrom are summarized in Table 4.

TABLE 4. Estimated average orientation angles and site I/site II distributions of BPDE bound covalently to different polynucleotides.

POLYNUCLEOTIDE	A'	θ_{BPDE}	%Site I	%Site II	X
(dG).(dC)					
(+)	-0.61[a]	43°	12	88	-0.022
(-)	0.44[b]	64°	90	10	-0.015
(dG-dC).(dG-dC)					
(+)	-0.80[a]	39°	10	90	-0.022
(-)	0.10[c]	57°	76	24	-0.0060
(dT-dC).(dA-dG)					
(+)	-0.21[a]	51°	30	70	-0.0056
(-)	0.04[c]	≈55°	≈100	--	--
(dA-dC).(dT-dG)					
(+)	-0.05[a]	≈55°	70	30	-0.014
(-)	no LD		≈100	--	--

[a]Evaluated at 346 nm. [b]Evaluated at 350 nm. [c]Evaluated at 355 nm.

For random orientations, or when $\theta_{BPDE} = 54.7^{o}$ (magic angle), $A' = 0$. In poly(dG-dC).(dG-dC) and poly(dG).(dC), the site II binding of (+)-*anti*-BPDE is characterized by angles of 39-43°; these values are close to those determined for (+)-*anti*-BPDE-DNA adducts [22,29]. The site I adducts are oriented with apparent angles of 57 - 64° in the alternating and non-alternating dG-dC polynucleotides; similar results were obtained with native DNA [22]. There was no discernable LD signal within the BPDE absorption band in adducts derived from the binding of (-)-*anti*-BPDE to the alternating pyrimidine-purine co-polymer poly(dA-dC).(dT-dG) (Fig. 7C). This suggests that the pyrenyl residues are randomly oriented. The adduct orientations in this polymer are also unusual in that the covalent binding of the (+)-enantiomer gives rise predominantly to a site I, rather than to the more usual site II orientations. Adducts derived from the binding of both *anti*-BPDE enantiomers to the non-alternating pyrimidine-purine co-polymer are somewhat better oriented (the $|A'|$ values are higher) than in alternating copolymer (Table 4), although the apparent orientation angles are quite close to the magic angle of ≈ 55°, probably implying a rather random degree of orientation.

Taken together, these results suggest that the covalently bound BPDE residues in the non-alternating (dG).(dC) and alternating (dG-dC).(dG-dC) co-polymers are

characterized by better defined carcinogen orientations than in the two co-polymers containing dA and dT nucleosides. Thus, the presence of dA-dT base pairs adjacent to dG-dC base pairs bearing covalent BPDE-N2-dG lesions, leads to a decrease in the apparent degrees of orientation of the carcinogen residues. In poly(dA-dT).(dA-dT) and poly(dA).(dT), covalently bound *anti*-BPDE enantiomers (presumably bound to N6 of dA, ref. 4) do not exhibit any linear dichroism signals (30). Thus, low degrees of BPDE residue orientations are associated with the presence of adjacent dA-dT base pairs.

The apparent lower degrees of orientation of BPDE residues covalently bound to dA residues or to dG residues with adjacent dA-dT base pairs may be due to the higher apparent flexibilities and decreased stiffness of polymers rich in (dA-dT) base pairs [31,32]. Furthermore, the base-pair opening or "breathing" rates are about ten times greater for dA-dT than for dG-dC base pairs (33). All of these factors suggest that the pyrenyl residues are more mobile when they are located in the vicinities of dA-dT base pairs; the apparent low degrees of average orientations measurable by the LD technique in poly(dT-dC).(dA-dG) and poly(dA-dC).(dT-dG), and a complete lack of orientation in poly(dA).(dT) and poly(dA-dT).((dA-dT) polymers, can thus be rationalized.

Analysis of Absorption and Linear Dichroism Spectra in Terms of Linear Combinations of Site I and site II Adduct Spectra.

It is of interest to determine how well the experimental LD and absorption spectra can be represented as simple linear sums of the site I and site II model absorption spectra shown in Fig. 4. In attempts to simulate the experimental absorption and LD spectra using the model absorption spectra shown in Fig. 4, we make use of the fact that the LD spectrum of a given adduct species is proportional to its absorption spectrum (Eq. 7). Therefore,

$$LD(\lambda) \approx f_{II}\,\varepsilon_{II}(\lambda) + X\, f_I\,\varepsilon_I(\lambda) \qquad [9]$$

$$A(\lambda) \approx A_I(max)\,\varepsilon_I(\lambda) + A_{II}(max)\,\varepsilon_{II}(\lambda) \qquad [10]$$

The variables $\varepsilon_I(\lambda)$ and $\varepsilon_{II}(\lambda)$ are the relative molar extinction coefficients (normalized to unity at the absorption maxima) of site I and site II which are depicted in Fig. 4. The factors f_I and f_{II} denote the fractions of molecules with site I and site II conformations. However, since base stacking interactions are important in site I adducts, while in site II conformations the pyrenyl residues are located in solvent-exposed conformations (23), the molar extinction coefficients of site I and site II adducts are expected to be somewhat different. Thus, the exact definitions of the f-factors are:

$$f_i = \frac{A_i(max)}{A_I(max) + A_{II}(max)} \qquad [11]$$

where the index i denotes either site I or site II, while $A_I(max)$ and $A_{II}(max)$ denote the absorbances at the site I and site II maxima (354 nm and 346 nm, respectively), which are proportional to the relative concentrations of these two adduct types. The factor X in Eq. [9] reflects the ratio of orientation factors for sites I and II, and is therefore always negative in sign:

$$X = \frac{3\cos^2\theta_I - 1}{3\cos^2\theta_{II} - 1} \qquad [12]$$

The fits of equations [9] and [10] to the experimental data (linear dichroism and absorption spectra) requires the use of only two unknown parameters (X and f_I or f_{II}, since $f_I + f_{II} = 1.0$), and the wavelength dependences of $_I(\ )$ and $_{II}(\ )$ which are provided in Fig. 4. The simplest approach to finding the closest simultaneous fits of Eqs. 9 and 10 to both the experimental linear dichroism and absorption spectra for a given set of parameters f_I (or f_{II}) and X, involved a simple trial and error method using a computer program. Only fairly unique sets of f_I and X values were found to approximate the LD and absorbance spectra simultaneously; these values are listed in Table 4. Good fits to the absorption spectra were not possible to attain in many cases. Nevertheless, this approach allows us to reach some conclusions concerning the utility and limitations of the site I - site II model of adduct conformations. All of the fits employing the parameters listed in Table 4 are shown in Figs. 5-8 (dotted lines).

As mentioned already, unoriented adducts, if present, contribute to the absorption but not to the linear dichroism spectra. Thus, the presence of such unoriented or poorly oriented adduct forms should be especially evident from differences between the simulated and the experimentally observed absorption spectra. Since unoriented adducts do not contribute to the LD spectra, much better agreement between simulated and experimental spectra are expected. Both expectations are indeed fulfilled (compare solid lines with dotted lines in Figs. 5-8.

Unoriented adducts should also give rise to small values of A' (Table 4). This seems to be the case in the poly(dA-dC).(dT-dG) polymer since A' = 0 for the (-) enantiomer, and nearly zero in the case of (+)-*anti*-BPDE (Table 4). The possibility that all of the adduct species are uniformly and fortuitously oriented at the magic angle of $\approx 55^o$ seems less likely. In contrast to poly(dA-dC)•(dT-dG), the relatively large values of A' for poly(dG).(dC) and poly(dG-dC).(dG-dC) suggest that the BPDE pyrenyl residues, on the average, possess a defined orientation with respect to the DNA bases.

Based on these simulated fits to the experimental linear dichroism and absorption spectra, several interesting conclusions can be reached. These are summarized for each polymer in the following paragraphs.

Poly(dG).(dC). The (-)-*anti*-BPDE-poly(dG).(dC) adducts can be closely approximated by the site I/site II model, since the differences between the experimental and simulated LD and absorption curves are modest. In the case of the (+)-*anti*-BPDE adducts, there is considerable more absorbance beyond 350 nm than is suggested by the LD spectrum; because of the large red shifts, these additional long-wavelength absorbing forms probably involve pyrenyl chromophores with significant base-stacking interactions. It was not possible to simultaneously fit the negative LD portion of the spectrum near 360 nm and the trough near 337 nm in Fig. 5D using the same sets of parameters. This suggests that the absorption spectra of the site I and site II forms in this polymer are somewhat broader than the model spectra shown in Fig. 4, at least in this polymer. The fractions of site II adducts obtained from these fits are 88%, while in the case of the (-)-adducts the site I adducts are more abundant (90%, Table 4).

Poly(dG-dC).(dG-dC). In the (-)-enantiomer case, the simulated LD and absorption spectra deviate quantitatively from the experimental spectra. There is little structure in the observed absorption spectrum, although a relatively sharp maximum occurs in the simulated absorption spectrum at 353 nm due to site I. This result indicates that the site I and site II absorption spectra in this polymer are also somewhat broader than the site I and site II model absorption spectra. The agreement between the simulated and experimental LD spectra are fairly reasonable (Fig. 6D), while the deviations in the absorption spectra are significant (Fig. 6B). The magnitude of the LD signal beyond 350 nm is much smaller than suggested from the rather prominent absorbances in this wavelength region. This shows up in the difference between the simulated and experimental absorption spectra and suggests that there is a significant fraction of long-wavelength, poorly oriented or unoriented site I-type adducts. The simulation suggests that the site II/site I oriented adduct ratio is 9:1 in the case of the (+)-adduct, and about 1:3 in the case of the (-)-adduct.

Poly(dT-dC).(dG-dA). The (-)-*anti*-BPDE adducts are best approximated by a homogeneous site I distribution. The experimental absorption spectrum is broader than the simulated one, while the reverse appears to apply in the case of the LD spectra (Figs. 7A and 7C, respectively). In the case of the (+)-adducts, the agreement between the simulated and experimental LD spectra are quite good (Fig. 7D), while the experimental absorption spectrum is significantly broader than the simulated one, especially in the long wavelength region (> 350 nm). The ratio of oriented site II/site I adducts is only 2.3 : 1, which is a much smaller ratio for the (+)-*anti*-BPDE enantiomer than in the poly(dG).(dC) and poly(dG-dC).(dG-dC) polymers (Table 4).

Poly(dT-dG).(dC-dA). There is no LD signal in the case of the (-)-adduct. In the case of the (+)-adduct, the simulated spectra shown in Figs. 8B and 8D were obtained with a site II/site I adduct ratio of only 0.4. This is the only polynucleotide (or DNA) which we have studied up till now, in which the (+)-*anti*-BPDE isomer gives rise predominantly to site I rather than to site II adduct conformations. Our HPLC data (Table 3) show that this effect cannot be attributed to a different chemical adduct distribution. This difference in the conformations of adducts is attributed to the effects of base-sequence.

CONCLUSIONS

(1) The site I - site II model, in all cases, provides a better description of the linear dichroism spectra than of the absorption spectra. This effect is due to the presence of unoriented or poorly oriented adduct forms, particularly in the polynucleotides containing the more flexible dA-dT base pairs. There are indeed two major classes of adduct sites, one with an absorption maximum at or near 346 nm (site I), and the other with a maximum near 354 nm (site II). The degrees of orientation of the bound pyrenyl residues are more pronounced in the alternating and non-alternating dG-dC polymers.

(2) The tumorigenic (+)-*anti*-BPDE isomer gives rise predominantly to external site II adducts, while the (-)-enantiomer gives rise predominantly to carcinogen-base stacked site I adducts. Comparisons with the chemical characteristics of these adducts (Table 3) suggest that site I adducts are *cis* in character, while site II adducts are *trans* in character. These conclusions are further supported by our results obtained with stereochemically specific BPDE-oligonucleotide adducts (described below).

while site II adducts are trans in character. These conclusions are further supported by our results obtained with stereochemically specific BPDE-oligonucleotide adducts (described below).

(3) In the mixed (dA-dC).(dT-dG) and (dT-dC).(dA-dG) co-polymers, the (+)-*anti*-BPDE isomer also binds predominantly to N2 of deoxyguanosine, but the adducts are only weakly oriented with respect to the DNA bases. The incidence of site II adducts is considerably reduced as compared to the (dG).(dC) and (dG-dC).(dG-dC) polymers, and there is a greater proportion of site I adducts. The presence of a significant proportion of unoriented adduct forms is suggested from the diffuseness and broadness of the absorption spectra in the dA-dT base pair-containing polymers.

(4) Finally, it is interesting to note that binding and mutational hot spots occur in sequences which are rich in dG-dC base pairs, especially those containing runs of dG's (25-28). Our studies indicate that the highly mutagenic (+)-*anti*-BPDE gives rise to well-oriented and well-defined site II adducts in non-alternating (dG).(dC) sequences. The correlation between the high tumorigenicity and mutagenicity of site II-type lesions have been previously noted (21). The presence of dA-dT base pairs near BPDE-dG binding sites gives rise to less well defined site II adduct orientations, and a higher proportion of site I, and of unoriented adduct species. We hypothesize that these effects may be related to the higher flexibilities, lower stiffness, and higher frequencies of base-pair opening of dA-dT base pairs.

B. CONFORMATIONS OF BPDE IN SINGLE-STRANDED AND DOUBLE-STRANDED POLYNUCLEOTIDES: DEVELOPMENT OF SENSITIVE DETECTION METHODS USING FLUORESCENCE.

Fluorescence Techniques for Probing Adduct Conformations.

In the previous section (A), we have shown how UV absorbance and linear dichroism techniques can be used to distinguish adducts of different conformations in different base sequences. Basically, these are low sensitivity techniques which are suitable for studying BPDE-DNA (or other types of PAH adducts) at modification levels of one BPDE residue (or more) per 1000 bases. *In vivo*, the level of binding varies from one BPDE residue per 20,000 bases, to one in 10^7 bases (reviewed in ref. 34). It is therefore highly desirable to develop sensitive methods for detecting BPDE-DNA adducts of different conformations (site I and site II, for example) in DNA samples derived from cells treated with BPDE or other carcinogens. We have shown recently that sites I and II can be distinguished by fluorescence methods [35,36].

Conformations of BPDE-dG and BPDE-dA adducts in single-stranded DNA.

The conformation of adducts in single-stranded DNA regions as, for example, at replication forks where DNA synthesis takes place, is of great interest. It is well established that *anti*-BPDE inhibits DNA elongation at replication forks [37], and gives rise to mutations in systems where BPDE-modified plasmids are allowed to replicate in human cells [27,38]. Fluorescence methods can provide information on the degree of base stacking interactions between aromatic carcinogens and DNA bases in single-stranded conformations.

Shifts in the absorption spectra of BPDE-nucleic acid adducts are accompanied by analogous shifts in the fluorescence excitation spectra (which resemble absorption spectra under ideal experimental conditions, e.g. when minor fluorescent impurities are absent). The fluorescence excitation and emission spectra of highly purified adducts derived from the covalent binding of (+)-anti-BPDE to the exocyclic amino group of *single-stranded* poly(dG) is shown in Fig. 10 (dashed lines). The fluorescence excitation maxima are significantly red-shifted as compared to BPT tetraols (in the absence of DNA): from 343 nm for BPT to 353 nm in (+)-BPDE-poly(dG) covalent adducts; similar effects are observed in the absorption spectra (data not shown). The fluorescence emission maxima are also red-shifted relative to those of BPT in solution, but only by 5 nm (from 379 & 399 nm for BPT to 384 & 404 nm for (+)-BPDE-poly(dG)). Similar effects are observed in adducts derived from the covalent binding of (+)-anti-BPDE to the exocyclic amino group of dA in the *single-stranded* polynucleotide poly(dA) (Fig. 11, dashed line).

Taken together, these red-shifted fluorescence excitation (and absorption spectra, data not shown) are similar to those of the site I-type adducts observed in the case of the double-stranded polymers. There are no classical intercalative binding sites in single-stranded DNA, but these relatively large red-shifted spectra (9-10 nm) suggest that significant $\pi - \pi^*$ base-stacking interactions are present; Upon heating these single-stranded BPDE-polynucleotide adducts, the red-shift is greatly diminished (from 9-10 nm to 1-3 nm, data not shown), as expected for such hydrophobic carcinogen-base stacking interactions in aqueous environments. Such stacking interactions are expected to seriously interfere with the normal DNA synthesis processes at the replication forks.

Changes in BPDE Adduct Conformations Upon Duplex Formation by Stoichiometric Titration with the Complementary Strands poly(dC) or poly(dT).

The fluorescence excitation and emission spectra of the resulting double-stranded adducts are shown in Figs. 10 and 11, respectively (solid lines). A striking change is observed when poly(dC) is stoichiometrically added to (+)-BPDE-poly(dG) adducts: the excitation maxima (and absorption maxima, data not shown), ***blue***-shift from 353 nm to 346 nm; in the double-stranded adducts the spectroscopic characteristics of the covalently bound BPDE residues correspond to those of site II (see above, section A). Thus, a striking conformational alteration occurs involving a change from carcinogen-base stacked conformations in single-stranded (+)-BPDE-poly(dG), to external site II adduct conformations in double-stranded (+)-BPDE-poly(dG)•(dC). In contrast, when the complementary strand poly(dT) is added to (+)-BPDE-poly(dA) adducts, the spectral changes are relatively minor (Fig. 11, solid lines); this indicates that carcinogen-base stacked conformations dominate in both the single-stranded (+)-BPDE-poly(dA) and the double-stranded (+)-BPDE-poly(dA)•(dT) polymers.

The covalent adducts derived from the less tumorigenic isomer (-)-*anti*-BPDE bound to single-stranded poly(dG), display similar base-stacking characteristics as those derived from the tumorigenic (+)-*anti*-BPDE shown in Fig. 10. However, there is no measurable and analogous blue-shift in the absorption or fluorescence excitation spectra when poly(dC) is added to (-)-BPDE-poly(dG) adducts. Thus, the striking conformational difference between single- and double-stranded poly(dG) adducts is confined to the tumorigenic (+)-BPDE. As shown in part A, the dominance of the external site II adducts in poly(dG-dC)•(dG-dC), poly(dG)•(dC), and native DNA, in the case of (+)-BPDE, seems to be peculiar to this highly tumorigenic isomer

and to double-stranded DNA conformations only. The implications of these findings are discussed further in a subsequent section dealing with oligonucleotide adducts.

Conclusions.

(1) Overall, based on the examples shown here and on other data, hydrophobic carcinogen-base stacking interactions are the rule in the case of single-stranded adducts, and covalent adducts derived from the non-tumorigenic (-)-*anti*-BPDE. External, site II conformations are formed efficiently only upon double-strand formation in the case of dG-dC polymers and the tumorigenic (+)-*anti*-BPDE.

(2) Fluorescence techniques are sensitive tools for distinguishing site I and site II adduct conformations even in cellular DNA. This has been demonstrated with DNA derived from Chinese hamster embryo cells treated with BPDE (to be published, R. Zhao, S.K. Kim, M. McLeod and N.E. Geacintov).

(3) Adducts involving binding of BPDE to dG or dA in nucleic acid polymers can be distinguished using the fluorescence R-ratio (the ratio of the 383/403 fluorescence emission intensities, [36,39]); this is evident from the results shown in Figs. 10 & 11: the R-ratio is 0.88 in (+)-BPDE-poly(dG)•(dC), while its value is 1.38 in (+)-BPDE-poly(dA)•(dT) double-stranded polymers. These same ratios are observed even in monomeric BPDE-dG and BPDE-dA adducts (data not shown here).

C. SYNTHESIS AND CHARACTERIZATION OF CARCINOGEN-OLIGONUCLEOTIDE ADDUCTS SITE-SPECIFICALLY MODIFIED AT SELECTED BASES AND POSITIONS.

Our studies of the interactions of BPDE with synthetic polynucleotides and analysis of the spectroscopic and chemical properties of the covalent adducts, pointed to the intriguing conclusion that *cis* and *trans* addition products are distinguished by different conformations. It was shown that *cis* and *trans* addition products involving the reaction of the exocyclic amino group of dG with the C10 position of BPDE, appear to be correlated with site I and site II adduct conformations which we have studied for many years [21,22]. We have also shown that site II adducts are always associated with the most tumorigenic diol epoxide isomers, while the less active isomers give rise to mixtures of site I and site II adduct conformations [21]. The differences in the biological activities of (+)-*anti*-BPDE and (-)-*anti*-BPDE can be rationalized based on these observations: the highly tumorigenic (+)-*anti*-BPDE stereoisomer upon binding to DNA gives rise predominantly to *trans* and to external site II adducts. The biologically less active (-)-enantiomer gives rise predominantly to *cis*, and thus to site I adduct conformations.

What are the physico-chemical and biochemical characteristics which distinguish site I and site II, or *cis* and *trans* adducts? In order to study this problem, it is necessary to study purified and authentic forms of *cis* and *trans* BPDE-N(2)dG adducts embedded in sequences of single- and/or double-stranded DNA. There is no known way to separate *cis* and *trans* adducts prepared from the reactions of BPDE stereoisomers with high molecular weight DNA or synthetic polynucleotides. In order to obtain such DNA adducts in pure form, we synthesized oligonucleotides of

defined base composition and sequence 9-11 bases long, and allowed these short DNA fragments to react either with (+)-BPDE or (-)-BPDE, to form covalent adducts.

BPDE-oligonucleotide Adduct Synthesis.

The oligodeoxynucleotides were synthesized using the phosphoramidite method and a Biosearch Cyclone automated DNA synthesizer (Milligen-Biosearch Corp., San Rafael, CA), and purified via OPC (oligonucleotide purification column, Applied Biosystems, Foster City, CA) and HPLC (Rainin Dynamax C_4 column). Concentrated solutions of oligonucleotides were then treated with BPDE; after completion of the reaction, the BPDE-oligonucleotides were separated from the unmodified oligonucleotides, tetraol and other reaction products via HPLC (reverse phase C_{18} columns). Details of the synthesis, purification, and adduct verification, will be published shortly [40], and thus will not be described further here.

Two examples of HPLC elution profiles, derived from two different oligomers d(ATACGCATA) and d(TATGCGTAT), are shown in Figs. 12a and 12b. These two polymers will be denoted by --CGC-- and --TGCGT--, respectively; the bottom traces in each figure were obtained by absorbance at 254, while the upper traces were obtained with a fluorescence detector (excitation 345 nm, viewing at 400 nm). The major adducts formed are *cis* and *trans* addition products (Fig. 13) involving the exocyclic amino group of guanosine and the C(10) position of BPDE. Using techniques described in [40], in the case of --CGC--, the elution peak at 23.0 min was found to be the *cis* adduct, while the higher peak at 24.4 min is due to the *trans* adduct. In the case of --TGCGT--, two small peaks and two larger peaks are observed, the smaller ones are attributed to *cis* adducts at the two different guanosines, while the larger peaks are due to *trans* adducts at the two different dG's. The larger peaks at 18-19 min are due to unmodified guanines. We have not yet identified which peak is attributable to one or the other guanosines, however this can be easily accomplished employing Maxam-Gilbert sequencing techniques since the molecular weights of the different fragments depends on where the BPDE residue is attached (work in progress). The percent of strands modified are 45% in the case of --CGC-- and 53% in the case of--TGCGT-- under these particular reaction conditions [40]. These yields are extraordinarily high and permit the synthesis of large quantities of BPDE-modified oligonucleotides for physico-chemical studies [40,41].

The *cis* and *trans* assignments are obtained by collecting the different eluates, subjecting the samples to enzyme hydrolysis, and by comparing the HPLC elution times of the *cis* and *trans* BPDE-N(2)dG adducts with those of authentic standards [18]. Typical circular dichroism of some BPDE-oligonucleotide adducts are shown in Fig. 14; the magnitude of the CD signal is noteworthy: the rather high molar ellipticity indicates that the CD spectrum is dominated by excitonic interactions between the transition moments of the guanosyl (μ_1) and pyrenyl (μ_2) residues [40]; the magnitude and wavelength dependence of the CD signal is proportional to the triple scalar product $R_{12} \cdot \mu_1 x \mu_2$, where R_{12} is the distance between the centers of the two moieties. The CD signal thus provides interesting information on adduct conformations and the changes in conformation brought about by double-helix formation, etc. This subject is under intensive investigation in our laboratory at this time; here we remark only that the CD spectra for these short oligonucleotides are basically due to the sum of BPDE-N(2)dG moieties and to smaller contributions from the base-stacking interactions between the DNA bases.

Base Sequence-dependence of Covalent Adduct Formation.

The possibility of synthesizing oligonucleotides of different sequences has provided us with an opportunity to investigate the probability of forming covalent addition products between (+)-anti-BPDE and guanosine in the sequence context 5'--**XGY**--3', where X and Y are either C, A or T. Additional experiments in which X and Y are G's are presently underway, and a preliminary result with X = Y = G is reported here. In these experiments, the nucleotide concentration was 9×10^{-4} M, the (+)-anti-BPDE concentration was 1.6×10^{-4} M, all other reaction and analytical conditions were as described elsewhere [40]. The per cent of strands of each sequence modified at dG are reported in Table 5.

TABLE 5. *Base sequence-dependence of per cent of strands modified covalently at dG with (+)-anti-BPDE.*

Oligonucleotide	Covalent modification, %
I. 11-mer (purines next to G*)	
d(CTATAGATATC)	10
d(CTATAGCTATC)	16
d(CTATCGATATC)	11
d(CTATTGATATC)	14
II. 11-mer (pyrimidines next to G*)	
d(CTATGGGTATC)	35 (or ≈ 12% average for each G)
d(CTATCGCTATC)	18
d(CTATTGTTATC)	21
d(CTATCGTTATC)	19
d(CTATTGCTATC)	17
III. 9-mers	
d(CTATGTATC)	21
d(TATGCGTAT)	26 (or ≈ 13% average for each G)
d(GATACATAG)	12 (or 6% average for each G)
d(GTATCGTAG)	29 (or 10% average for each G)
d(GATGCATATG)	23 (or ≈ 8% average for each G)

--**XGY**--, central triplet in bold-face to stress effects of neighboring bases X and Y on reactivities with the central dG.

Conclusions.

(1) The presence of A at the 3'-side of the modified G is characterized by the lowest reactivities.

(2) Guanines at the ends of the chains are less reactive than those surrounded by pyrimidines or purines.

(3) The presence of the pyrimidines C and T at both sides of G leads to the highest reaction yields.

(4) In the case of the --GGG-- oligonucleotide, the HPLC profiles suggest that two of the G's are 3.5-4 more highly modified than the third, but we have not yet had time to perform Maxam-Gilbert sequencing experiments to determine which of the three G's is least modified.

(5) The *trans/cis* adduct ratios in all cases lie in the range of 3.4-5.0; there is some apparent sequence-dependence, but the effect is not strong.

(6) There is no difference in reactivities in either 9-mers or 11-mers containing a single G residue.

(7) Small yields of binding of BPDE to adenosine residues are also observed. However, we have not yet studied these minor adenine adducts in detail.

(8) The efficiencies of modification of G are a function of base sequence and decreases in the order:

$$CGC \geq TGT \approx CGT \approx TGC > AGC > CGA$$

We speculate that the presence of the bulky purine A on either side of target G base, hinders the approach of the reactive end of the BPDE molecule, i.e. the C(10) position, towards the N(2) moiety of guanine, thus lowering the covalent reaction yield. If this reasoning is correct, than the central G in the sequence --GGG-- will turn out to be the least modified (see (4) above).

(9) Separate experiments in which we measured reaction yields of (+)-*anti*-BPDE to single-stranded d(ATATGTATA) and double stranded d(ATATGTATA)•(TATACATAT) showed that the single G in the double-stranded form was 5 times less reactive than in the single-stranded form under the same conditions! These results are consistent with previous observations that, under certain conditions, the covalent binding yield of racemic *anti*-BPDE to denatured DNA is about twice as high as that to native, double-stranded DNA [42]. Apparently, the reaction geometry is not optimal in the noncovalent, pre-reaction intercalation complexes in double-stranded DNA. This further confirms the view (Part I of this report) that intercalation complex formation in native DNA is not critical for the covalent binding reaction between BPDE and the exocyclic amino group of guanosine.

Electrophoretic Mobilities of Modified Oligonucleotides.

In order to verify the accuracy of the oligonucleotide sequences produced by the DNA synthesizer, we set up high resolution Maxam-Gilbert sequencing gels [43]. It is of interest to also determine the relative electrophoretic mobilities of different BPDE-modified oligonucleotides. It was previously shown that racemic BPDE introduces a kink at the DNA binding site [44], while more recently it was suggested that (+)-*anti*-BPDE introduces such a kink or flexible joint, while (-)-*anti*-BPDE does not [29]. All of these experiments were done with high molecular weight DNA or synthetic polynucleotides. The availability of highly defined BPDE-oligonucleotide adducts offers us the possibility of carrying out electrophoretic mobility experiments on *cis* and *trans* (+)- and (-)-*anti*-BPDE-oligonucleotide adducts. DNA bending can be explored by gel electrophoresis [45], since bent DNA fragments tend to migrate slower than straight ones.

(single-stranded d(CACATG*TACAC) modified covalently with BPDE at the starred G) are compared for (left to right): (+)-trans, (+)-cis, unmodified 11-mer, (-)-trans, and (-)-cis. The different spots are labeled; the additional, higher mobility (lower) spots are believed to be due to radiation degradation products of the initially pure sequences used, and can thus be ignored.

The (+)-trans adduct is unique among the four since it migrates the slowest. The other three adducts migrate at the same rate, but slower than the unmodified 11-mer. By comparing these mobilities to those of a dA ladder, it can be demonstrated that (+)-*trans* migrates like a 13.6-mer, while the other three adducts migrate as 13-mers. The molecular weight of a BPDE residue is 302; thus, if there were no conformational changes, and since the electrical charge of the BPDE residue is zero, all adducts are expected to migrate approximately as 12-mers in the absence of other conformational effects. Since all adducts migrate visibly slower than a 12-mer, a conformational change, which is most pronounced in the case of the (+)-*trans*-adduct, manifests itself. This change could be a hinge joint [46], or a bend. Thus, there is a unique structural feature in these single-stranded adducts generated from *trans* addition of (+)-*anti*-BPDE, which is not observed in the case of the (+)-*cis* adducts, or (-)-BPDE adducts.

The difference in electrophoretic gel mobilities between (+)-*trans* and (+)-*cis* adducts in the 9-mer d(ATATG*TATA) is demonstrated in Fig. 15B. Again, the (+)-*trans* adduct displays the slowest mobility. These differences in electrophoretic mobilities are likely to depend on the base-sequence surrounding the modified G. This effect is now being studied, since a highly flexible or rigid BPDE-dG lesion at or near the replication fork could have different consequences. It will be interesting to determine if the mutagenic (+)-*trans* adducts behave similarly in the case of other highly tumorigenic PAH diol epoxide molecules.

Characteristics of BPDE-oligonucleotide Adducts: cis and trans Adducts Correspond to Site I and Site II Conformations.

The oligonucleotides used in this work are only 9-11 base pairs long, and therefore cannot be oriented in the hydrodynamic flow gradients of our Couette cells for linear dichroism analysis. However, as we have demonstrated above, the same kind of information can be obtained by absorption or fluorescence excitation spectra. Site I spectra with pseudo-intercalation structures exhibit red-shifted absorption maxima (maxima at 353 and 354 nm). Site II adducts located at the exterior of DNA double-helices are characterized by absorption maxima near 345 - 346 nm. We present here some representative results obtained with covalent BPDE-d(CACATG*TACAC) adducts, where the starred guanosine denotes the location of the covalently linked BPDE residue. This particular sequence was selected because of favorable characteristics for future NMR studies.

In Fig. 16 A, it is shown that remarkable conformational changes are occurring when single-stranded *trans*-BPDE-oligonucleotide adducts are titrated with the complementary strands. The absorption spectrum of (+)-*trans*-BPDE-d(CACATGTACAC) exhibits an absorption maximum at 350 nm, which is close to the maximum observed in the case of the (+)-BPDE-poly(dG) adducts as we discussed above. Upon adding the complementary strand d(GTGTACATGTG) to form the double-stranded (+)-*trans*-BPDE-d(CACATGTACAC)•(GTGTACATGT) adduct, there is a distinctive ***blue-shift*** in the absorption maximum from 350 nm to 346 nm! Similar behavior was observed when the

complementary strand d(GTGTACATGTG) to form the double-stranded (+)-trans-BPDE-d(CACATGTACAC)•(GTGTACATGT) adduct, there is a distinctive ***blue-shift*** in the absorption maximum from 350 nm to 346 nm! Similar behavior was observed when the complementary poly(dC) was added to single-stranded (+)-BPDE-poly(dG) adducts (Fig. 10); in the latter case, both *cis* and *trans* adducts are present, although chemical analysis shows that *trans*-adducts dominate in the case of the (+)-enantiomer of BPDE. Performing similar titration experiments with (+)-*cis*-BPDE-d(CACATGTACAC) adducts does ***not*** produce a blue-shift upon duplex formation: the single-stranded adduct exhibits an absorption maximum at 352 nm, which merely shifts to 353 nm upon duplex formation (Fig. 16 B).

Single-stranded (+)-*trans*-BPDE-oligonucleotide adducts are characterized by strong pyrenyl residue-base stacking interactions which are accompanied by red-shifted (relative to free BPT tetraols) absorption maxima at 350 nm. Upon addition of complementary (unmodified strands), a duplex is formed and the pyrenyl residue is forced outside of the double-helix and into the aqueous exterior (site II), thus resulting in a blue-shift (4 nm) in the absorption spectrum. In the case of the (+)-*cis*-BPDE-oligonucleotides, the pyrenyl residues are base-stacked in both the single-stranded and the double-stranded forms; therefore, there is little change in the absorption spectrum upon duplex formation.

While we have discussed one specific example to demonstrate this behavior, the results are quite general and are observed also with (-)-BPDE-oligonucleotide adducts (Fig. 16). On the basis of these observations we have proposed the hypothesis that ***trans-BPDE-DNA adducts give rise to exterior site II conformations, while cis-BPDE adducts give rise to site I conformations*** [41]. Since the occurrence of site II adducts is associated with highly tumorigenic and mutagenic stereoisomers of PAH diol epoxides [21], this hypothesis can be further extrapolated to state that ***trans-BPDE-DNA lesions are biologically more deleterious than cis-BPDE-DNA lesions,*** possibly because of differences in adduct conformations (site I and site II). This working hypothesis will be tested further with BPDE and other PAH diol epoxides. In the next few pages we provide a short summary of BPDE-oligonucleotide adduct characterizations and base-sequence effects obtained to date, which point the way to further exciting studies.

Thermodynamics of Double-Helix Formation: Influence of Covalent cis and trans BPDE Adducts.

Typical melting profiles of the double-stranded adducts d(CACATG$\overset{*}{G}$TACAC)•(GTGTACATGTG), where the starred G* contains a covalently bound (+)-*anti*-BPDE, or (-)-*anti*-BPDE residue bound at N(2) of dG, either *cis* or *trans*, are shown in Fig. 17. The total strand concentration was C_T = 3 μM in this set of experiments. All melting curves suggest that a two-state equilibrium (single <---> double strands) is appropriate in all cases. The unmodified strand (Fig. 17 A) has a melting point of T_{m_o} = 43° C, the (+)-*trans* adduct 30°, the (+)-*cis* adduct 37°, the (-)-*trans* adduct 24°, and the (-)-*cis* adduct 21°. It is evident that the covalently bound residue destabilizes the double-helices; the less tumorigenic (-)-*anti*-BPDE seems to destabilize double-helix formation more than the (+)-isomer. Also, the (+)-*cis* adduct imparts a greater stability to the modified double-stranded oligonucleotides than the (+)-*trans*-BPDE. However, the melting points T_m are concentration-dependent, and thus a more detailed analysis is required to assess the thermodynamics of the single strand - double strand equilibrium.

We consider the equilibrium between single-stranded (ss) and double-stranded (ds) oligonucleotides (duplex formation):

$$ss + ss \underset{}{\overset{K_{duplex}}{\rightleftharpoons}} ds \qquad [13]$$

where K_{duplex} is the equilibrium constant for duplex formation. If α is the fraction of strands in the duplex form, then:

$$K_{duplex} = 2\alpha/[C_T(1 - \alpha)^2] \qquad [14]$$

It is known that at or close to the melting point of the duplexes, T_m, the value of $\alpha = 0.41$ [47]. From the equation:

$$\Delta G^o = \Delta H^o - T_m \Delta S^o = -RT_m \ln K_{duplex} \qquad [15]$$

it can be shown that [47]:

$$1/T_m = (R/\Delta H^o)\ln C_T + (1/\Delta H^o)(\Delta S^o - 1.71) \qquad [16]$$

and that the enthalpy change ΔH^o and entropy change ΔS^o accompanying duplex formation can be evaluated from studies of the dependence of T_m on the total strand concentration C_T. Plots of $1/T_m$ vs. $\ln C_T$ were found to be linear indicating that the enthalpy and entropy changes are temperature-independent in the temperature range of 15 - 60° C (data not shown). The values of ΔH^o and ΔS^o deduced from such plots are summarized in Table 6.

TABLE 6. ***Thermodynamic characteristics of duplex formation of unmodified d(CACATGTACAC) and BPDE-modified d(CACATG*TACAC) with the complementary strands (GTGTACATGTG).***

Strand	ΔG^o	ΔH^o	ΔS^o	$\Delta\Delta S^o$
unmodified	-12.4	-86.0	-247	--
(+)-trans	-9.4	-90.7	-273	-26
(+)-cis	-10.7	-95.5	-284	-37
(-)-trans	-8.4	-29.7	-72	+145
(-)-cis	-8.7	-19.5	-38	+205

ΔG^o and ΔH^o in units of kcal/mole, ΔS^o in cal/deg-mol, evaluated at 298 K. $\Delta\Delta S^o$: entropy of modified DNA minus unmodified DNA cases.

There are striking differences between the adducts derived from the tumorigenic (+)-*anti*-BPDE and non-tumorigenic (-)-*anti*-BPDE. The (+)-adducts produce a more favorable enthalpy change, but the less favorable free energy terms (and thus K_{duplex}) arise from less favorable entropy terms in the presence of the hydrophobic adducts; thus, the more favorable enthalpy changes are outweighed by the more negative entropy changes. In the case of the (-)-BPDE adducts, there is a severe decrease in the magnitude of the negative enthalpy change, but a more favorable

entropy term is observed (ΔS^o is less negative in the presence of bound (-)-BPDE than in the case of the unmodified strands).

The difference in entropy changes (as compared to the unmodified case), is only 10-15% for the (+)-adducts. However, the $\Delta\Delta S^o$ values are +105 to 205 cal/deg mol in the case of the (-)-adducts; these values are much larger than the entropy changes observed upon intercalation of polycyclic aromatic compounds (Table 1), and suggest that severe perturbations of the normal double helical DNA structure are caused by the presence of the covalently bound (-)-*trans* and (-)-*cis* BPDE residues.

In order to understand these thermodynamic effects, we are presently conducting base sequence dependent studies in which the nature of the base pairs around the dG* sites are being varied. At this time, pending additional studies, we refrain from possible detailed interpretations of the observed changes in the thermodynamic parameters. However, it is clear that covalently bound (-)-BPDE residues are more disruptive than (+)-BPDE residues. We speculate that the more massive alterations caused by the (-)-*anti* isomer of BPDE might represent efficient replication blocks or invoke efficient DNA repair processes *in vivo*; in either case, mutations are not expected to arise. The less dramatic changes accompanying adduct formation in the case of the (+)-BPDE isomer, might allow the lesions to persist up to the replication fork, where error-prone replication processes might occur. The putative differences in biological activities between the (+)-*trans* and (+)-*cis*-BPDE-DNA adducts may be a function of steric rather than thermodynamic factors. These speculative remarks can be tested by performing site-directed mutagenesis experiments with such sterically defined lesions incorporated into genomes of phages or plasmids replicated in suitable host cells [48]. It is hoped that thorough characterizations of sterically and chemically defined BPDE-DNA adducts in our laboratory, as well as in others, will stimulate such experiments in the future.

Double Strand Formation with a Mismatched Base Opposite the BPDE Lesion.

The carcinogen 2-aminofluorene (AF) bound to the C(8) position of guanosine induces predominantly G•C ---> T•A transversions [49]. A recent NMR study shows that a complementary strand with A, rather than the normal C opposite the 2-[(N-deoxyguanosin-8-yl)aminofluorene lesion forms a stable duplex [50]. This finding suggests that the observed mutational specificity could be due to the preferred incorporation of A opposite the (AF)G lesion during replication.

In the case of racemic *anti*-BPDE, the dominant observed point mutations also involve G•C ---> T•A transversions [27,38]. We have therefore examined the possibility that the BPDE-oligonucleotide single-strands form preferably duplexes with complementary strands with a mismatched base opposite the BPDE-N(2)dG lesion. Some examples of melting profiles with mismatched complementary strands are shown in Fig. 18. In the case of (+)-*trans*-BPDE-d(CACTG*TACAC), addition of the natural complementary strand (GTGACATGTG) gave rise to the most stable duplexes. The melting points T_m decreased in the following order when C opposite the BPDE-N(2)dG lesion was replaced by another base: **A** > **G** ≈ **T**. In the case of the (+)-*cis* adduct, the positioning of **C**, rather than **A**, opposite the lesion, also resulted in a more stable duplex (Fig. 18). Thus, we conclude that base mispairing during replication is less likely in the case of BPDE than in the case of AF, at least from a point of view of thermodynamic stability.

Computer-generated Models of BPDE-dG Lesions and Comparisons with Experimental Data.

This aspect of the work is being conducted in collaboration with Dr. Suse Broyde at NYU and Dr. Brian Hingerty at Oak Ridge. We are sharing one theoretical graduate student, Suresh Singh, in this part of the project. Up till now, we have considered in detail only trans-BPDE-N(2)dG adducts built into alternating dG-dC sequences. Recent experimental data described earlier in this report, point to the importance of the differences in conformation of *trans* and *cis* adducts; therefore, our present efforts are focused on an understanding of the differences between these *cis* and *trans* adducts. Here, we summarize our almost completed work with the *trans* *anti*-BPDE-dG lesions with the pyrenyl residues lying in the minor groove.

Using the DUPLEX algorithm (running on the DOE Cray X-MP and Cray-2 at Livermore, CA and on the NSF Cray X-MP at San Diego), in which torsion angle space is variable and solvent and salt effects are treated indirectly, two different low-energy conformations were identified:

(I) The pyrenyl plane is approximately parallel to the planes of the bases, the modified guanine is displaced from its normal position in the helix, one base pair is denatured, and the other base pairs are intact forming an overall Watson-Crick type B-DNA helix. This conformation has all of the characteristics of the experimental ***site I*** binding sites.

(II) The pyrenyl moiety lies in the minor groove, all base pairs are intact and of the Watson-Crick type, forming a B-DNA helix. These characteristics are consistent with those of ***site II***.

These two minimum energy conformations for each of the two BPDE enantiomers were used as starting points in a 100 ps molecular dynamics simulation. The presence and participation in the dynamics of solvent and salt were explicitly taken into account employing the AMBER force field. Unlike DUPLEX in which the torsional parameters are variable, in AMBER all Cartesian coordinates are variable. Due to constraints in our available computational resources, the sequence $d(G-C)_6 \cdot (G-C)_6$, with the G at the 7th position from the 5' side modified trans at N(2) was employed in this work. A simulation using a similar unmodified DNA duplex was also carried out as a control. One of the starting (external, site II) (+)-trans-BPDE-N(2)dG structures generated by DUPLEX is shown in Fig. 19. The other starting structure involved (-)-trans-BPDE-N(2)dG in a site I conformation (not shown).

Important conformational movements in these structures were observed within the first 50 ps. In the (-)*trans*-BPDE-$d(G-C)_6 \cdot (G-C)_6$ adduct case, the pyrenyl residue is initially protruding into the major groove. After 50 ps, the flat pyrene ring system had moved into an intercalative conformation forming a hydrogen bond between the C8-hydroxyl group of the BPDE residue and N4 of dC which normally would have been the Watson-Crick partner of the modified dG residue. Further movements in the 50-100 ps range were much less pronounced.

In the case of the (+)*trans*--BPDE-$d(G-C)_6 \cdot (G-C)_6$ minor-groove structure shown in Fig. 19, the pyrene residue is stacked with a guanine base on the partner strand and on the 3'-end of the modified dG residue. A hydrogen bond between the C8-OH group of BPDE and the exocyclic $-NH_2$ group of a guanine base on the opposite strand and on the 5'-side of the lesion is observed. In the dynamic simulations, large movements are observed initially; the most striking change involves the rupture of

the base pairs on the 5'-side, but not on the 3'-side of the lesion. As the dynamic evolution proceeds, the helix becomes more bent at the lesion than at the beginning; at the end of the simulation, the pyrenyl residue (long axis) is oriented at an average angle of about 20° to the axis of the helix defined by the unmodified base pairs. The large initial movements may well be due to rearrangements of the energy minima generated with DUPLEX by the explicit presence of solvent and salt in the AMBER force field.

Comparisons of these structures with experimental data show that the (+)-*trans*-BPDE-d$(G\text{-}C)_6 \cdot (G\text{-}C)_6$ model (minor groove structure, Fig. 19) has all of the attributes of the experimentally determined site II conformation; the characteristics which are alike are the following: (1) orientation of the pyrenyl residue, (2) exposure to water, and (3) helix bend at the site of the lesion. The carcinogen-base stacked structure is similar to the experimental site I conformation due to analogous orientations of the pyrenyl residue and smaller degree of solvent exposure.

The experimental results summarized in Table 4 indicate that both (+)-BPDE and (-)-BPDE, upon binding covalently to poly(dG-dC).(dG-dC) give rise to a mixture of both site I and site II conformations. While site II conformations are heavily favored in the case of the (+)-isomer, the ratio of site I/site II adducts is similar in the case of (-)-BPDE. We have concluded above that *trans* adducts in both cases have site II conformations. This is in full accord with the predictions of the DUPLEX results, which predict that both *anti*-BPDE enantiomers are characterized by adducts in which external conformations, rather than carcinogen-base stacked structures have the lowest energies. The preference of the less tumorigenic (-)-*anti*-BPDE to form carcinogen-base stacked adducts, is due to the high incidence of *cis* addition products, which prefer site I adduct conformations. We are now in the process of carrying out the molecular dynamics simulations with *cis* BPDE-N(2)dG adducts as well, in order to determine if these experimental results can also be predicted from computer modelling studies.

The thermodynamic data summarized in Table 6, suggests that there are significant differences between the double-stranded (+)-trans and (-)-trans-BPDE-oligonucleotide adducts. On the other hand, the minor groove models suggest that the extent of perturbations of the double-helix are rather similar in the case of the (+)-*trans* and the (-)-*trans* adducts. The DUPLEX procedure has actually shown that a major groove, external (-)-trans-BPDE adduct is energetically also feasible and is characterized by significantly greater structural perturbations than in the case of the minor groove (-)-*trans* adducts. In contrast, there are no low-energy conformations of the (+)-*trans* adduct in the major groove. The intriguing possibility that the (+)-*trans* adduct resides in the minor groove, while the (-)-*trans*-BPDE adduct prefers a major groove conformation, is presently being investigated in detail.

REFERENCES

1. Dipple, A., Moschel, R.C. and Bigger, C.A.H. (1984) in: *Chemical Carcinogens*, C.A. Searle, Ed., ACS Monograph 182, Vol. 2, 41-163 (1984).
2. Hingerty, B.E. and Broyde, S. (1985) *Biopolymers* 24, 2279-2299 (1985).
3. Hingerty, B.E. and Broyde, S. (1986) *J. Biomol. Struct. Dynamics* 3, 365-372.
4. Geacintov, N.E., Yoshida, H., Ibanez, V. and Harvey, R.G. (1981) *Biochem. Biophys. Res. Commun.* 100, 1569-1577.

5. Meehan, T., Gamper, H.and Becker, J.F. (1982) J. Biol. Chem. 257, 10470-10485.
6. Roche, C.J., Geacintov, N.E., Ibanez, V. and Harvey, R.G. (1989) *Biophys. Chem.* 33, 277-288.
7. Geacintov, N.E., Shahbaz, M., Ibanez, V., Moussaoui, K. and Harvey, R.G. (1988) *Biochemistry* 27, 8380-8387.
8. LeBreton, P.R. (1985) in: *Polycyclic Hydrocarbons and Carcinogenesis* (R.G. Harvey, Ed.) ACS Symposium Series 283, 209-238.
9. McLeod, M.C., Smith, B. and McClay, J. (1987) *J. Biol. Chem.* 262, 1081-1087.
10. Shimer, G.H. Jr., Wolfe, A. and Meehan, T. (1988) *Biochemistry* 27, 7960-7966.
11. Abramovich, M., Prakash, A.S., Harvey, R.G., Zegar, I.S. and LeBreton, P.R. (1985) *Chem.-Biol. Interactions* 55, 39-62.
12. Urano, S., Fetzer, S., R.G. Harvey, R.G., Tasaki, K. and P.R. LeBreton, P.R. (1988) *Biochem. Biophys. Res. Commun.* 154, 789-795.
13. Shahbaz, M., N.E. Geacintov and R.G. Harvey (1986) *Biochemistry* 25, 3290-3296.
14. Carberry, S.E., Shahbaz, M., Geacintov, N.E. and Harvey, R.G. (1988) *Chem. Biol.-Interactions* 66, 121-145.
15. Geacintov, N.E., Waldmeyer, J., Kuzmin, V.A. and Kolubayev, T. (1981) J. *Phys. Chem.* 85, 3608-3613.
16. Poulos, T., Kuzmin, V.A. and Geacintov, N.E. (1982) *J. Biochem. Biophys. Methods* 6, 269-281.
17. Conney, A.H. (1982) *Cancer Res.* 42, 4875-4917.
18. Cheng, C.C., Hilton, B.D., Roman, J.M. and Dipple, A. (1989) *Chem. Res. Toxicol.* 2, 334-340.
19. Brookes, P. and Osborne, M.R. (1982) *Carcinogenesis* 3, 1223-1226.
20. Harvey, R.G. and Geacintov, N.E. (1987) *Accts. Chem. Res.* 21, 66-73.
21. Geacintov, N.E. (1988) in *Polycyclic Aromatic Hydrocarbon Carcinogenesis: Structure-Activity Relationships."* Yang, S.K. and Silverma, B.D., Eds., CRC Press, Boca Raton, FL, Vol. II, pp. 181-206.
22. Geacintov, N.E., Ibanez, V., Gagliano, A.G., Jacobs, S.A. and Harvey, R.G. (1984) *J. Biomol. Structure and Dynamics* 1, 1473-1484.
23. Kolubayev, V., Brenner, H.C. and Geacintov, N.E. (1987) *Biochemistry* **26**, 2638-2641.
24. Gräslund, A. and Jernström, B. (1989) *Quart. Rev. Biophys.* 22, 1-37.
25. Boles, T.C. and Hogan, M.E. (1986) *Biochemistry* **25**, 3039-3043.
26. Kootstra, A., Lew, L.K., Nairn, R.S. and MacLeod, M.C. (1989) *Mol. Carcinogenesis* 1, 239-244.
27. Yang, J.-L., Maher, V.M. and McCormick, J.J. (1987) *Proc. Natl. Acad. Sci. USA* **84**, 3787-3791.
28. Reardon, D.B., Bigger, A.C.H., Strandberg, J., Yagi, H., Jerina, D.M. and Dipple, A. (1989)
29. Erikssen, M., Nordén, B., Jernström, B. and Gräslund, A. (1988) *Biochemistry* **27**, 1213-1221.
30. Roche, C.J. (1988) Ph.D. Dissertation, New York University.
31. Hogan, M.E. and Austin, R.H. (1987) *Nature (London)* **329**, 263-266.
32. Sarai, A., Mazur, J., Nussinov, R. and Jernigan, R.L. (1989) *Biochemistry* **28**, 7842-7849.
33. Kochoyan, M., Leroy, J.L. and Guéron, M. (1987) *J. Mol. Biol.* **196**, 599-609.
34. Geacintov, N.E. (1988) *Progress in Analytical Luminescence*, D. Eastwood and L.J. Cline-Love, Eds., American Society for Testing and Materials, Philadelphia, pp. 54-66.
35. Kim, S.K., Geacintov, N.E., Brenner, H.C. and Harvey, R.G. (1989) *Carcinogenesis* 10, 1333-1335.

36. Kim, S.K., Geacintov, N.E., Zinger, D. and Sutherland, J.C. (1989) in *Synchrotron Radiation in Structural Biology. Basic Life Sciences., Vol. 51*, R.M. Sweet and A.D. Woodhead, Eds., Plenum Press, New York, pp. 187-205.
37. Paules, R.S., Cordeiro-Stone, M., Mass, M.J., Poirier, M.C., Yuspa, S.H. and Kaufman, D.G. (1988) *Proc. Natl. Acad. Sci. USA* **85**, 2176-2180.
38. Maher, V.M., Yang, J.-L., Mah, C.-M. and McCormick, J.J. (1989) Mutat. Res. **220**, 83-92.
39. Kim, S.K., Brenner, H.C., B.-J. Soh and Geacintov, N.E. (1989) *Photochem. Photobiol.* 50, 327-337.
40. Cosman, M., Ibanez, V., Geacintov, N.E. and Harvey, R.G. (1990), *Carcinogenesis*, in press.
41. Geacintov, N.E., Cosman, M., Ibanez, V., Birke, S.S. and C.E. Swenberg, in: *Molecular Base Specificity in Nucleic Acid-Drug Interactions.* B. Pullman and J. Jortner, Eds., Kluwer Academic Press, Dordrecht, 1990, in press.
42. Geacintov, N.E., Zinger, D., Ibanez, V., Santella, R., Grunberger, D. and Harvey, R.G. (1987) *Carcinogenesis 8*, 925-935.
43. Maxam, A.M. and Gilbert, W. (1977) *Proc. Natl. Acad. Sci. USA* 74, 560-564.
44. Hogan, M.E., Dattagupta, N. and Whitlock, J.P., Jr. (1981) *J. Biol. Chem. 256*, 4504-4513.
45. Crothers, D.M. (1987) Nature 325, 464-465.
46. Schwartz, A., Marrot, L. and Leng, M. (1989) *J. Mol. Biol. 207*, 445-450.
47. Gaffney, B.L. and Jones, R.A. (1989) *Biochemistry 28*, 5881-5889.
48. Basu, A.K. and Essigman, J.M. (1988) *Chem. Res. Toxicol. 1*, 1-18.
49. Carothers, A.M., Steigerwalt, R.W., Urlaub, G., Chasin, L. and Grunberger, D. (1989) *J. Mol. Biol. 208*, 417-428.
50. Norman, D., Abuaf, P., Hingerty, B.E., Live, D., Grunberger, D., Broyde, S. and Patel, D.J. (1989) Biochemistry *28*, 7462-7476.

PUBLICATIONS SUPPORTED BY THIS PROJECT (1988-1990).

1.* "Intercalation and binding of carcinogenic hydrocarbon metabolites to nucleic acids." R.G. Harvey and N.E. Geacintov, *Accts. Chem. Res. 21*, 66-73 (1988).

2.* "Applications of fluorescence techniques in the analysis of polycyclic aromatic carcinogen-DNA adducts." N.E. Geacintov, in: ***Progress in Analytical Luminescence***, D. Eastwood and L.J. Cline-Love, Eds., American Society for Testing and Materials, Philadelphia, pp. 54-66 (1988).

3.* "Mechanisms of reaction of polycyclic aromatic epoxide derivatives with nucleic acids." N.E. Geacintov, in: ***Polycyclic Aromatic Hydrocarbon Carcinogenesis: Structure-Activity Relationships***, Vol. 2, S.K. Yang and B.D. Silverman, Eds., CRC Press, Inc., Boca Raton, FL, pp. 181-206 (1988).

4.* "Reactions of stereoisomeric and structurally related bay region diol epoxide derivatives of benz[a]anthracene with DNA. Conformations of non-covalent complexes and covalent adducts." S.E. Carberry, M. Shahbaz, N.E. Geacintov and R.G. Harvey, *Chem.-Biol. Interactions 66*, 121-145 (1988).

5. "Base-sequence dependence of noncovalent complex formation and reactivity of benzo[a]pyrene diol epoxide with polynucleotides." N.E. Geacintov, M. Shahbaz, V. Ibanez, K. Moussaoui and R.G. Harvey, *Biochemistry 27*, 8380-8387 (1988).

6. "Linear dichroism properties and orientations of different ultraviolet transition moments of benzo[a]pyrene derivatives bound noncovalently and covalently to DNA." C.J. Roche, N.E. Geacintov, V. Ibanez and R.G. Harvey, *Biophys. Chem. 33*, 277-288 (1989).

7. "Reactions of stereoisomeric non-bay region benz[a]anthracene diol epoxides with DNA and conformations of noncovalent complexes and covalent adducts." S.E. Carberry, N.E. Geacintov and R.G. Harvey, *Carcinogenesis 10*, 97-103 (1989).

8. "Fluorescence spectral characteristics and fluorescence decay profiles of covalent polycyclic aromatic carcinogen-DNA adducts." S.K. Kim, N.E. Geacintov, D. Zinger and J.C. Sutherland, in: ***Synchrotron Radiation in Structural Biology***, Basic Life Sciences, Vol. 51, R.M. Sweet and A.D. Woodhead, Eds., Plenum Press, New York, pp. 187-205 (1989).

9. "Differences in conformation of covalent adducts derived from the binding of 5- and 6-methylchrysene diol epoxide stereoisomers to DNA." N.E. Geacintov, M.-S. Lee, V. Ibanez, S. Amin and S.S. Hecht, *Carcinogenesis 11*, 985-989 (1990).

10. "Characteristics of noncovalent and covalent interactions of (+) and (-) *anti*-benzo[a]pyrene diol epoxide stereoisomers of different biological activities with DNA." N.E. Geacintov, M. Cosman, V. Ibanez, S.S. Birke and C.E. Swenberg, in: ***Molecular Basis of Specificity in Nucleic Acid-Drug Interactions***, B. Pullman and J. Jortner, Eds., Kluwer Academic Publishers, Dordrecht, in press (1990).

SUBMITTED

11. "DNA base sequence dependence of conformations of adducts derived from the covalent binding of enantiomers of benzo[a]pyrene diol epoxide of different tumorigenicities to DNA." C.J. Roche, A.M. Jeffrey, B. Mao, A. Alfano, S.K. Kim and N.E. Geacintov (9/90).

IN PREPARATION

"Molecular dynamics simulations of oligomer guanine N^2 - (+) and (-)-*anti*-benzo[a]pyrene diol epoxide adducts with solvent and salt." S.B. Singh, N.E. Geacintov, B.E. Hingerty, J. Greenberg, C. Singh and S. Broyde (10/90).

"Thermodynamics of duplex formation of benzo[a]pyrene diol epoxide-modified deoxyoligonucleotides." M. Cosman and N.E. Geacintov (10/90).

"Stereospecificity and conformations of adducts formed from the reactions of (+)- and (-)-*anti*-benzo[a]pyrene diol epoxides with poly(dG)•(dC) and poly(dG-dC)•(dG-dC)." B. Mao, A. Alfano, S.K. Kim. V. Ibanez and N.E. Geacintov (11/90).

---

*Publications acknowledging support from contract DE-AC02-78EV04959, the preceding project period, but which appeared in print during 1988.

PERSONNEL ASSOCIATED WITH THIS GRANT

Research Associates:

Dr. Y. Mnyukh

Research Assistants:

S. Singh
L. Balasta
S. Carberry
L. Juszczak
C. Roche

Undergraduate Students:

L. Pecaro

High School Students (Westinghouse Talent Search Program):

W. Lee
S. Chan

Visiting Scientists:

Dr. V.A. Kuzmin, Moscow, USSR Academy of Sciences.
Dr. S. Smirnov, Moscow, USSR Academy of Sciences
Dr. J. Deprez, Paris, IUT, Paris.

DISSERTATIONS.

S.E. Carberry, Ph.D., 1988.
C.J. Roche, Ph.D., 1988.
M.-S. Lee, Ph.D., 1989.

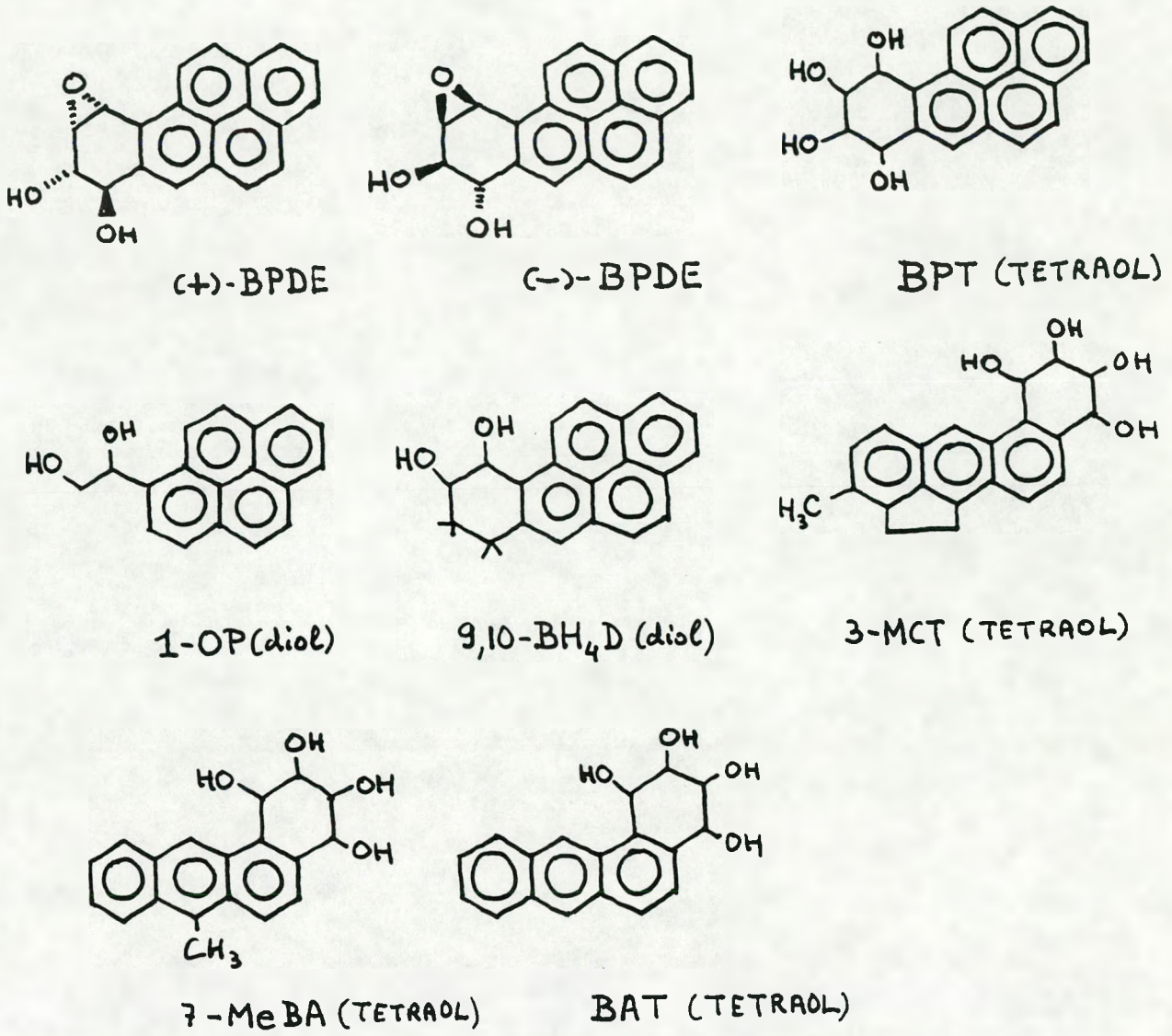
(+)-BPDE
(−)-BPDE
BPT (TETRAOL)
1-OP(diol)
9,10-BH4D (diol)
3-MCT (TETRAOL)
7-MeBA (TETRAOL)
BAT (TETRAOL)

Fig. 1.

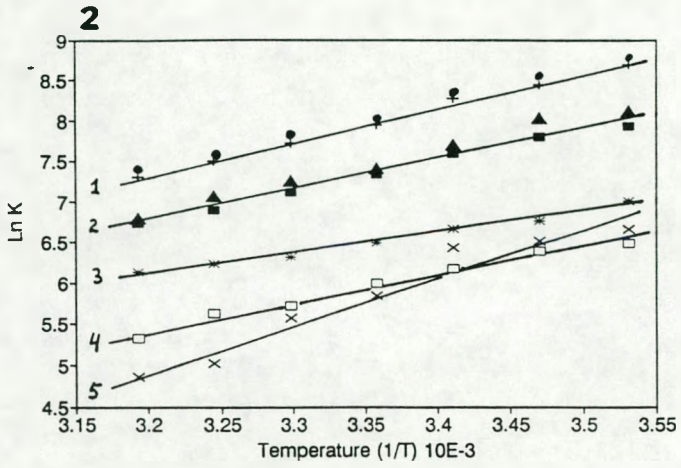

Fig. 2. Van't Hoff plots of noncovalent association constant K to DNA. 1..1-OP diol and 9,10-BPH$_4$D(cis), 2..BPT and 9,10-BPH$_4$D(trans), 3..MCT, 4..7-MeBA (#1), 5..7-MeBA (#2).

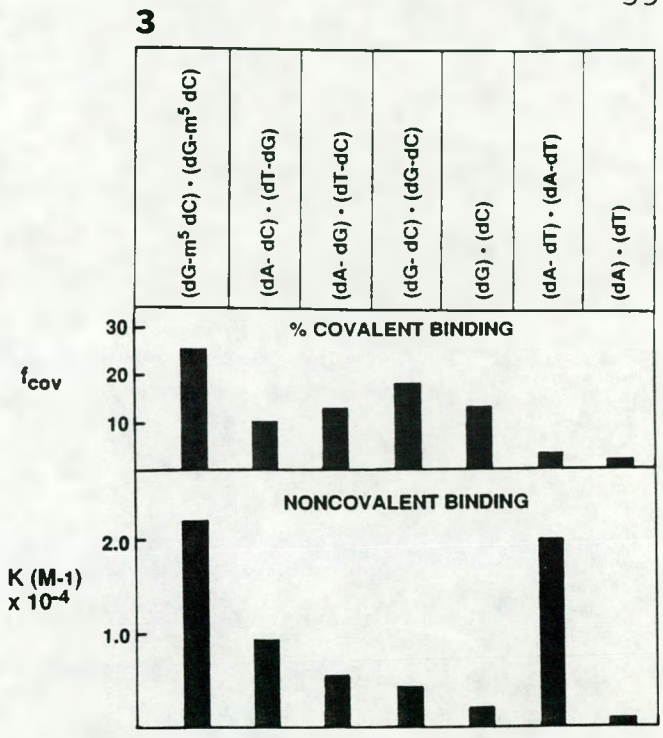

Fig. 3. Base sequence dependence of noncovalent binding (K) and covalent binding (f_{cov}).

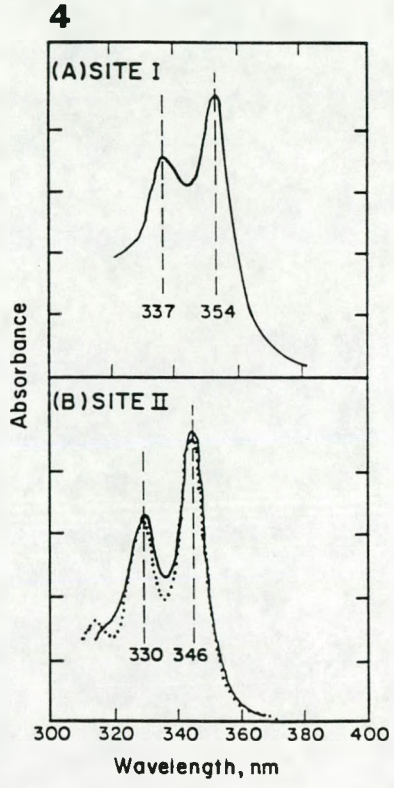

Fig. 4. Site I and Site II absorption spectra.

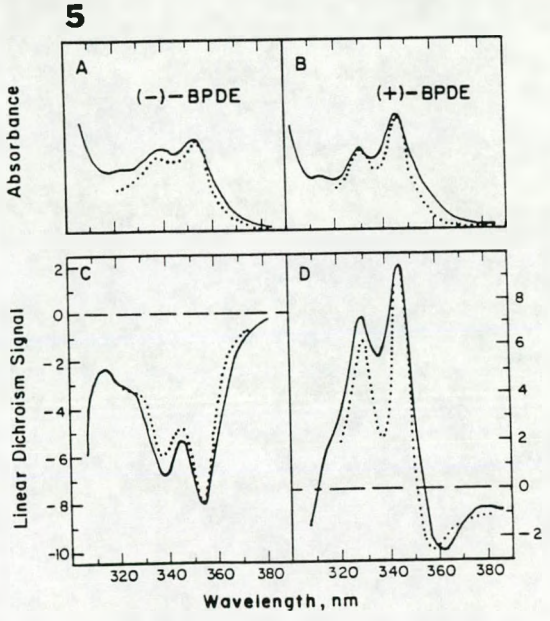

Fig. 5. Absorption and LD spectra. Poly(dG)•(dC).

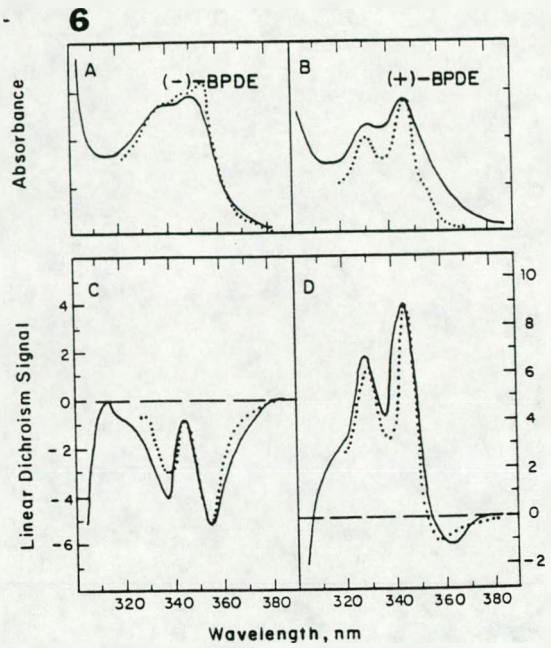

Fig. 6. Absorption and LD spectra. Poly(dG-dC)•(dG-dC).

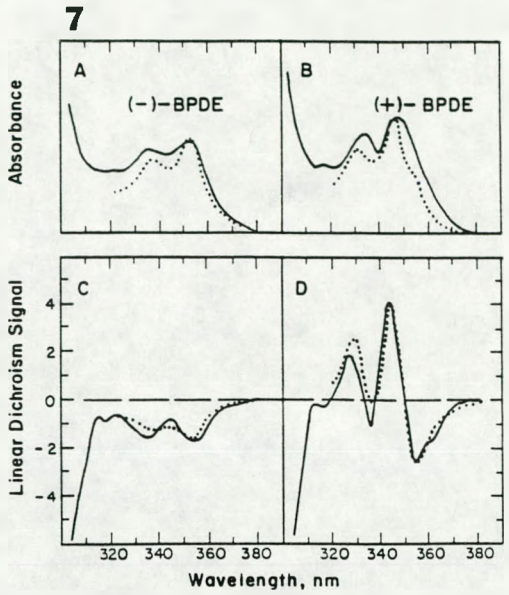

Fig. 7. Absorption and LD spectra. Poly(dT-dC)•(dA-dG).

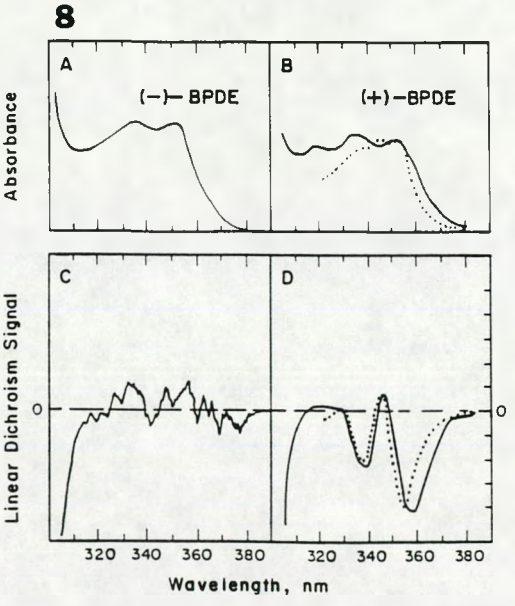

Fig. 8. Absorption and LD spectra. Poly(dT-dG)•(dA-dC).

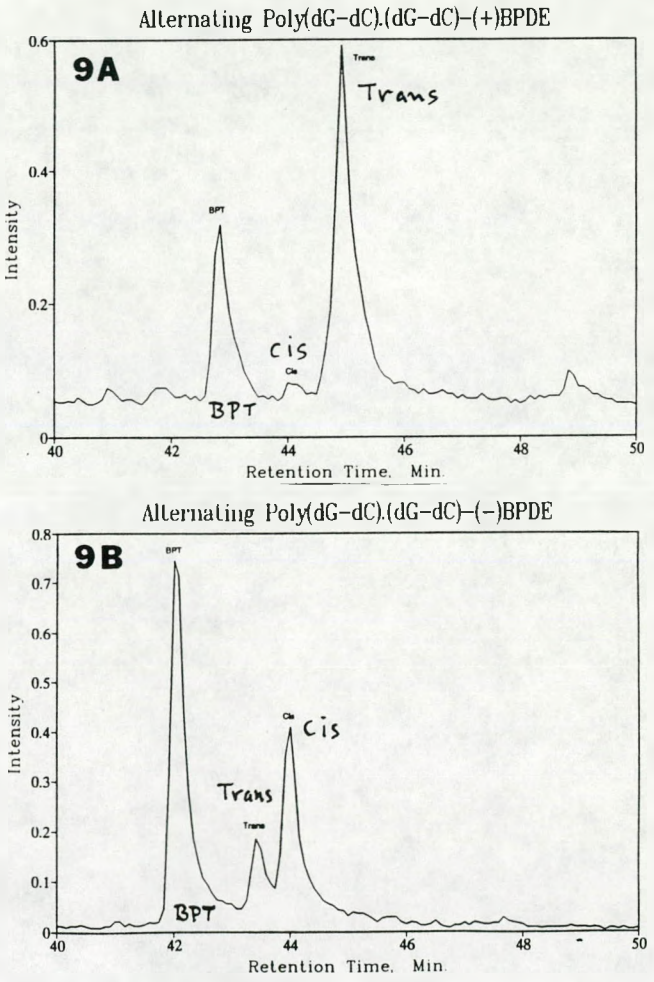

Fig. 9. Fluorescence-detected HPLC profiles.

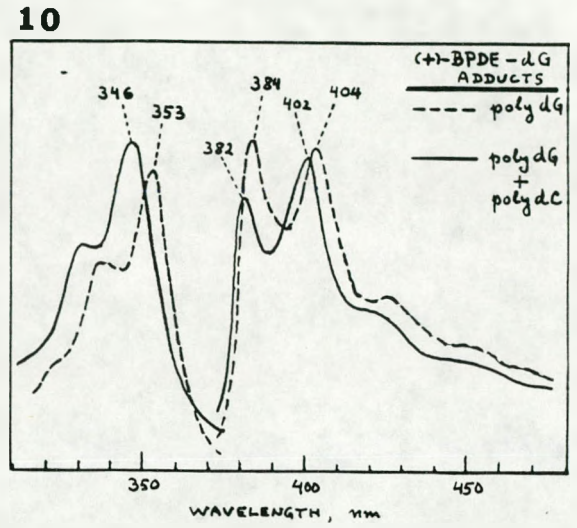

Fig. 10. Fluorescence excitation (left) and emission spectra (right).

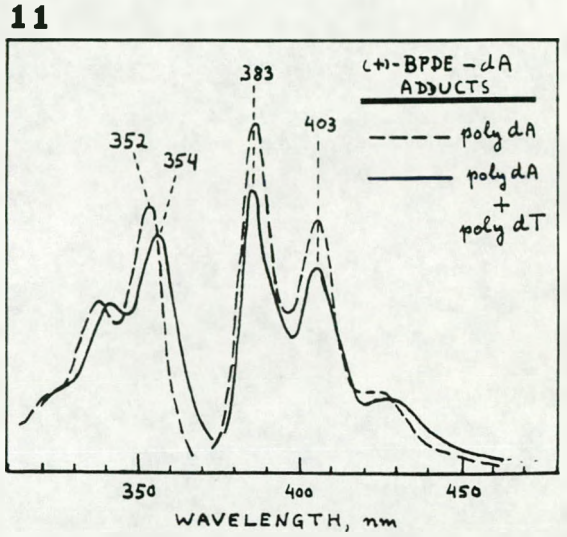

Fig. 11. Fluorescence emission (left) and emission spectra (right).

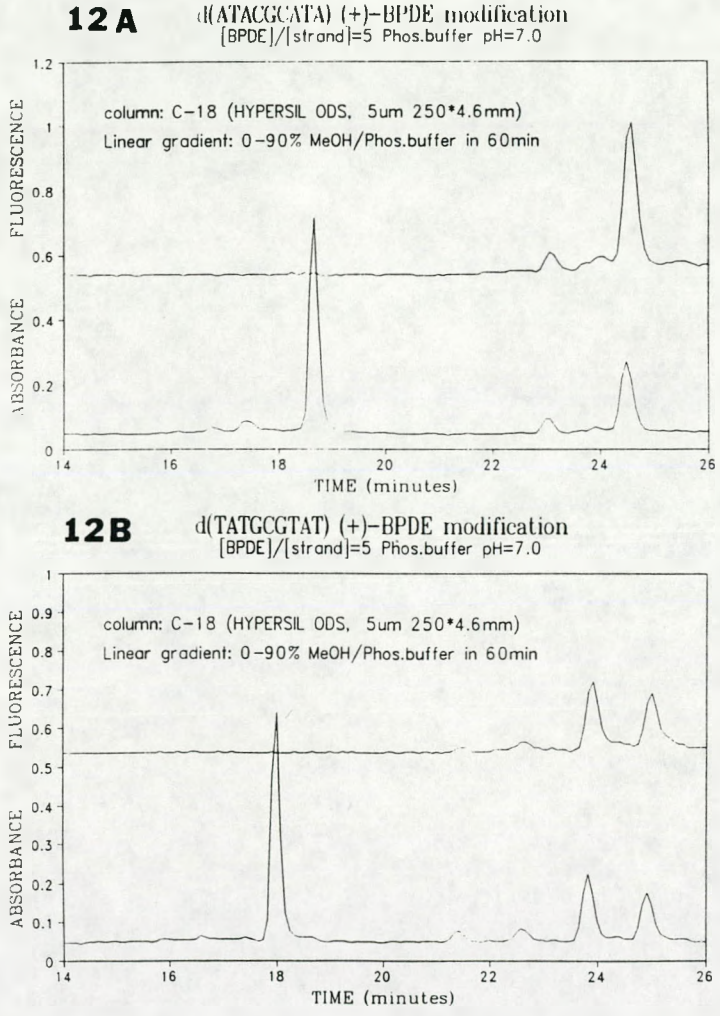

Fig. 12. HPLC elution profiles; fluorescence detection, upper curve in each figure; UV absorbance, lower traces.

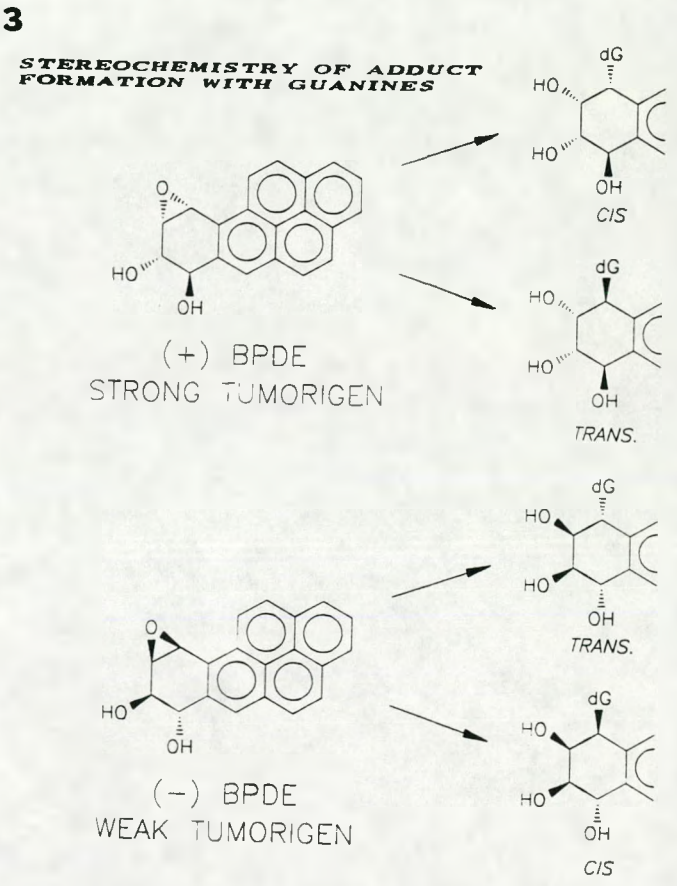

Fig. 13. Stereochemistry of adduct formation.

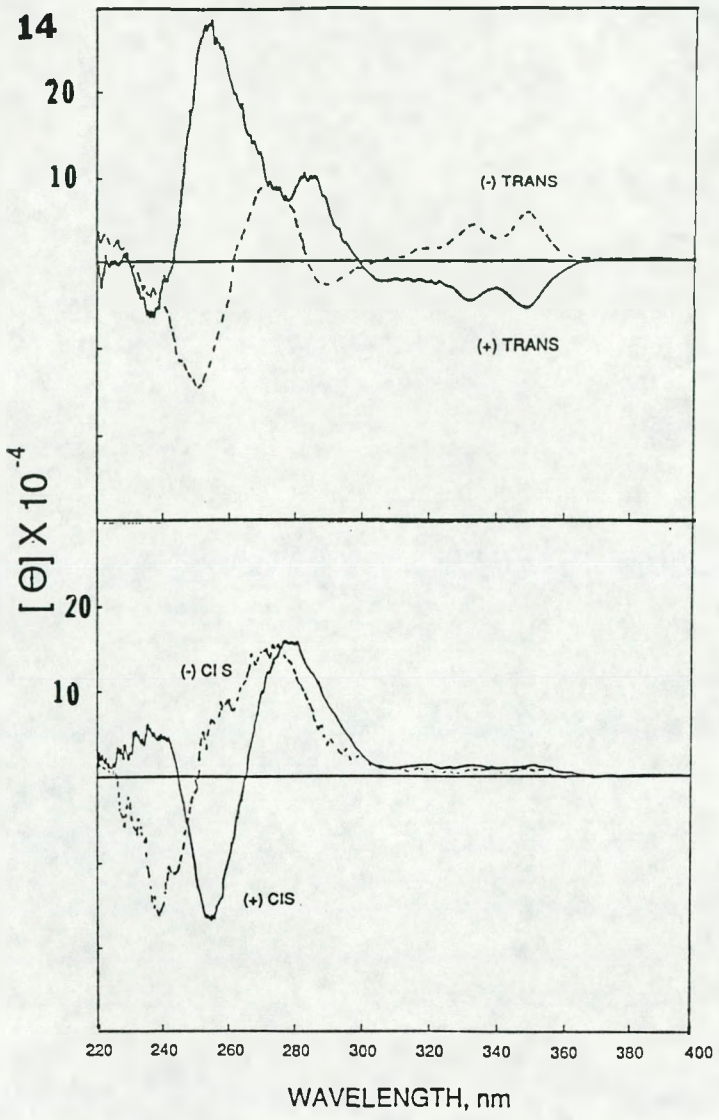

Fig. 14. CD spectra of adducts.

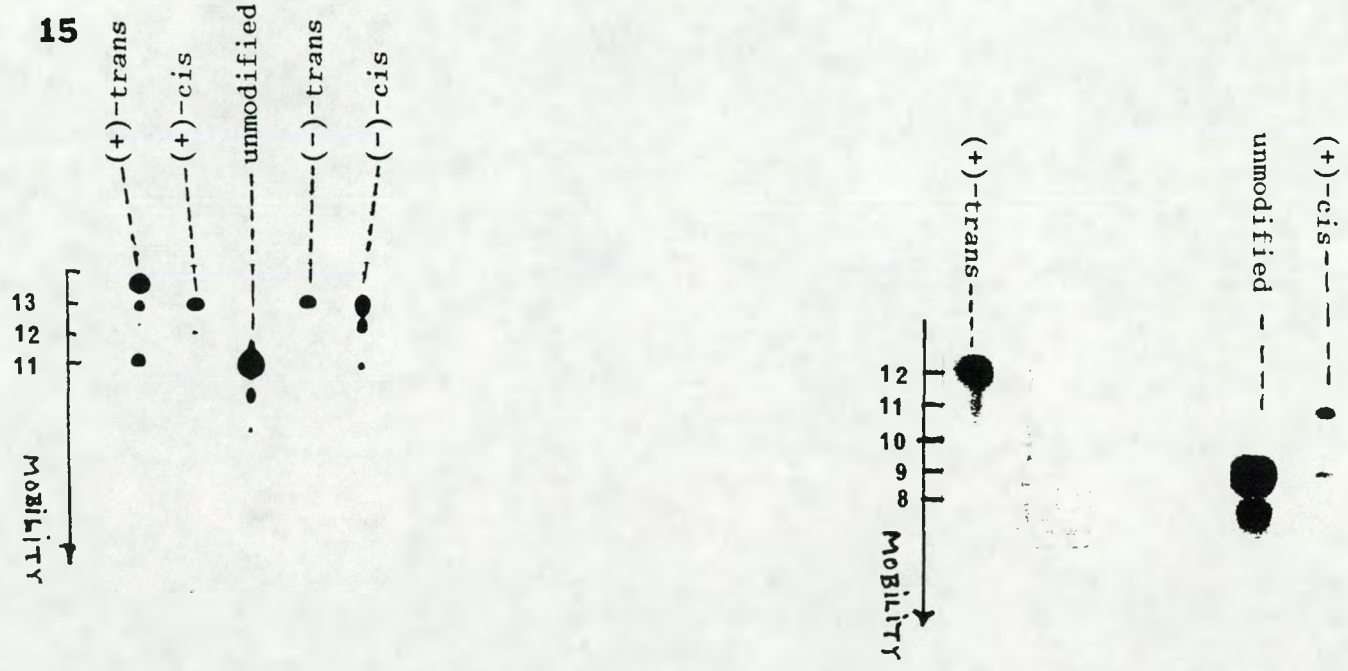

Fig. 15. Electrophoresis on 20% polyacrylamide gels. Left: 11-mer adducts; right: 9-mer adducts. The approximate equivalent length in number of bases is indicated on the vertical scales.

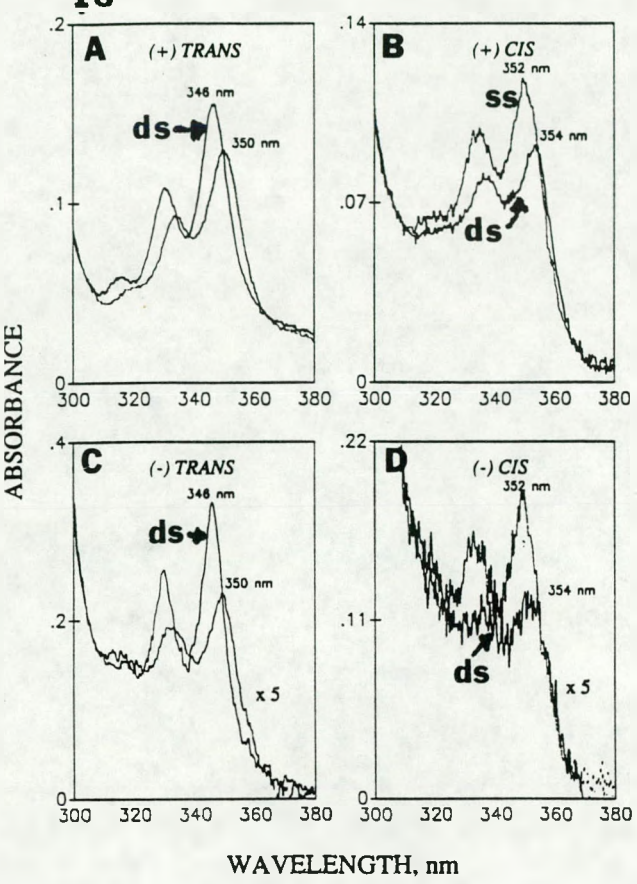

Fig. 16. Absorption spectra of adducts in single-stranded (ss) and double-stranded forms.

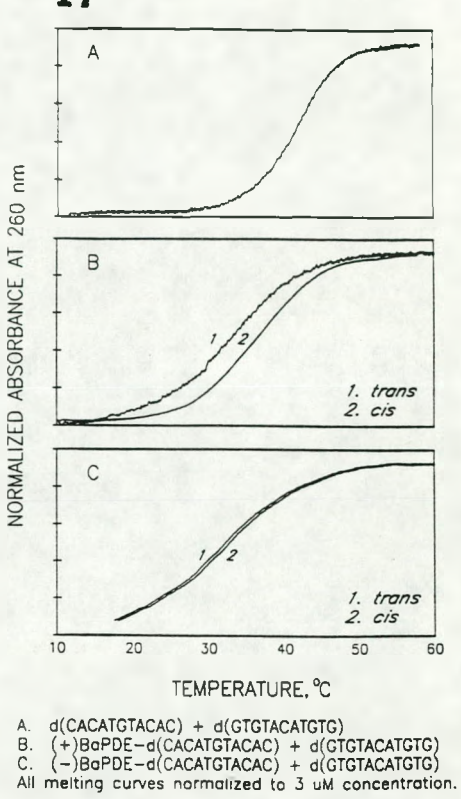

Fig. 17. Melting curves of duplexes; natural complementary strands.

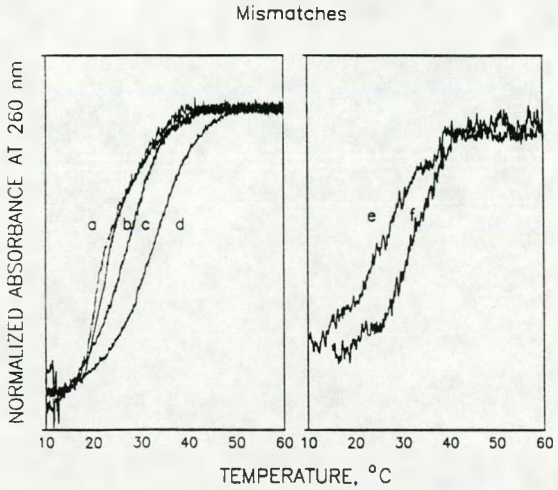

Fig. 18. Melting curves: noncomplementary strands.

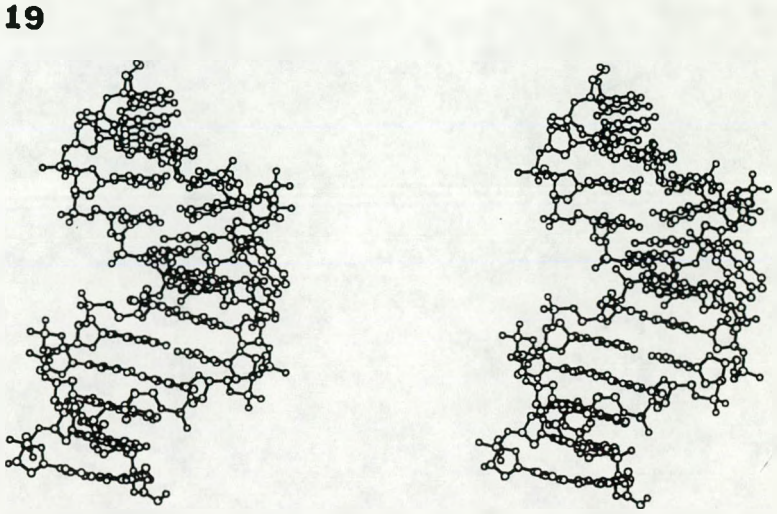

Fig. 19. Stereo-view of BPDE-N(2)dG adduct in a $(dG\text{-}dC)_6 \cdot (dG\text{-}dC)_6$ sequence.